Republic of Iraq
Ministry of Higher Education
and Scientific Research
University of Babylon
College of Education for Pure Sciences
Department of Physics

Preparation of Chlorophyll Bio-filler and Study their Effect on Structural and Optical Properties of some Bio Polymer Blends

A Thesis

Submitted to the Council of the College of Education for Pure Sciences, University of Babylon in Partial Fulfillment of the Requirements for the Degree of Master in Education / Physics

By

Ahmed Hussein Arar Kazem
B. E. Sc. (Physics)
(University of Babylon 2009)

Supervised by

Prof. Dr. Sameer Hassan Hadi Alnesrawy

2023 A.D **1445 A.H.**

بسم الله الرحمن
الرحيم

(قُل لَّوْ كَانَ
ٱلْبَحْرُ مِدَادًا
لِّكَلِمَٰتِ رَبِّى لَنَفِدَ
ٱلْبَحْرُ قَبْلَ أَن
تَنفَدَ كَلِمَٰتُ رَبِّى
وَلَوْ جِئْنَا بِمِثْلِهِ

Dedications

To the one who spent his life with an inexhaustible gift in my life

My martyr father

To a blessing that God honored me with

My dear mother

To my life mates and my soul mate

My brothers and sisters

To a supporter who is always next to me, the companion of her prayers

My big sister Wijdan

To the one who stood beside me in this journey with every step, and to the one who will continue the journey of my life with

Ahmed…

Acknowledgements

In the Name of Allah, the Compassionate, the Merciful First, thanks to Allah, the Lord of earth and heaven for completing my research, then, I would like to express my deep gratitude and appreciation to my supervisor, ***Prof. Dr. Sameer Hassan Alnesrawy*** *for suggesting this project, guidance, support, and encouragement through the research work. Thanks to the deanship of the College of education for Pure Sciences- University of Babylon and the Department of Physics for offering me the opportunity to complete my research. I also would like to express gratitude to all teachers, instructors and students of department of physics for their assistance and supports specially* ***Prof. Dr. Shurooq Sabah Abdullabbas*** *and* ***Prof. Dr. Ahmed Hashim Mohaisen*** *for encouragement and support.*

Thank you very much to my close friends who always supported me and helped me and eased the difficulties that I faced while working, ***Safa, Zainab,*** *and* ***Muhannad,*** *and finally thanks to everyone who helped me in one way or another during the preparation of this dissertation. I apologize to those I missed mentioning. I wish everyone success.*

Ahmed…

Summary

In this study, the (CMC-PVA/Mg-Chlorophyll) and (CMC/PVP/Mg-Chlorophyll) nanocomposite has been prepared by using casting method with variant content of Mg-Chlorophyll nanoparticles (2, 4, 6 and 8) wt.%. The structural, morphological and optical properties of (CMC-PVA/Mg-Chlorophyll) and (CMC-PVP/Mg-Chlorophyll) nanocomposite have been investigated. The structural properties include X-ray diffraction (XRD), optical microscope (OM), field emission scanning electron microscope (FESEM) and Fourier transformation infrared ray (FTIR).

The XRD obtained that the semicrystalline structure of CMC-PVA and CMC-PVP polymer blend and with added different concentration of Mg-Chlorophyll Pigments (2, 4, 6 and 8 wt.%), the intensity increased and there are no peaks appears, which due to the low concentration added to the CMC-PVA and CMC-PVP polymer blend and also due to the broad peaks of the CMC-PVA and CMC-PVP which disappear all peaks.

From the optical microscope and Field Emission Scanning Electron Microscope the images showed the Mg-Chlorophyll) form a continuous network inside the CMC-PVA and CMC-PVP polymer blend at concentration of 8 wt.%.

FTIR spectra shows shift in some bonds and change in the intensities and proved that there are no interactions between the CMC-PVA and CMC-PVP polymer matrix and Mg-Chlorophyll nanoparticles.

The optical properties exhibited that the absorbance, absorption coefficient, extinction coefficient, refractive index, real and imaginary parts of dielectric constants and optical conductivity are increased with increasing the concentration

of Mg-Chlorophyll nanoparticles, while the transmittance and the indirect energy gap decreased with the increasing concentration of Mg-Chlorophyll nanoparticles. application of the (CMC-PVA/Mg-Chlorophyll) and (CMC-PVP/Mg-Chlorophyll) nanocomposite for attenuation of electromagnetic waves .

Contents		
No	***Subject***	***Page***
	Dedication	I
	Acknowledgments	II
	Summary	III
	Contents	V
	List of Table	VIII
	List of Figures	IX
	List of Symbols	XII
	List of Abbreviations	XIII
Chapter One ***Introduction and Literature Review***		
1.1	Introduction	1
1.2	Polymer Structure	2
1.3	Classification of Polymers	3
1.3.1	Thermal classification of polymers	3
1.3.2	Structural classification of polymers	4
1.3.3	Polymers dependent on homogeneity	5
1.4	Polymer Blends	6
1.5	Biopolymer	6
1.6	Composite Materials	6
1.7	Materials Used in The Study	8
1.7.1	Polyvinyl Alcohol (PVA)	8
1.7.2	Carboxymethyl Cellulose (CMC)	9
1.7.3	Polyvinyl Pyrrolidone (PVP)	11
1.7.4	Mg-Chlorophyll Pigments	12

List of Tables

List of Symbols	
Symbol	***Physical Meanings***
θ_β	Bragg diffraction angle of the XRD peak (degree)
A	Absorbance
B	Constant according to the type of material
c	Velocity of light
d	the distance can be determined
D	Average crystallite size
E	Energy
E_{opt}	Energy gap
E_{ph}	Energy of phonon
ε	Dielectric constant
ε_1	Real dielectric constant
ε_2	Imaginary dielectric constant
h	Plank constant
i	Imaginary number
$I_\circ$	Incident Intensity of Light
I_A	Absorbed light
I_T	Transmitted rays
K_o	Extinction Coefficient
n	Refractive Index
N	Complex refractive index
r	Exponential constant (according to the type of transition).
R	Reflectance

r_o	Radius of bubble
t	Thickness
T	Transmittance
α	Absorption coefficient
B	Full width at half maximum of the peak
γ	Surface tension
λ	Wavelength of light
σ_{op}	Optical Conductivity
List of Abbreviations	
Symbol	***Physical Meanings***
PVP	Polyvinyl pyrrolidone
PVA	Poly vinyl alcohol
CMC	Carboxymethyl Cellulose
FTIR	Fourier Transformation Infrared Ray
FFSEM	Field emission scanning electron microscope
OM	Optical Microscopy
UV	Ultraviolet
OMCs	Organic matrix composites
MMCs	Metal matrix composites
CMCs	Ceramic matrix composites
PMCs	Polymer matrix composites

Chapter One

Introduction and

Literature Review

1.1 Introduction

Since ancient times, polymers have been used on a large scale, and among the oldest known polymers at that time are polymers of natural origin (cellulose, leather), which consist mainly of polymers[1].

In the nineteenth century, contrary to what some believe, the composition of polymers was unknown until two centuries ago, when scientists sought to determine how these materials were formed, and to seek to establish a way to achieve their artificial manufacture [1]. The first time the term "polymers" was used was in 1833, thanks to the Swedish chemist Jöns Jacob Berzelius, who used it to refer to substances of an organic nature having the same empirical formula but different molar masses. After some experiments to obtain synthetic polymers from the transformation of natural polymeric species, the study of these compounds gained more importance. The purpose of these investigations was to optimize the already known properties of these polymers and obtain new materials that could fulfill specific purposes in various fields of science [2]. In the twentieth century Scientists noticed that the rubber was soluble in a solvent of an organic nature, and then the resulting solution showed some unusual properties, and the scientists were worried and did not know how to explain them. From these observations, they conclude that materials like this exhibit very different behavior from smaller particles, as they can see while studying rubber and its properties [3]. From these observations, they conclude that materials like this exhibit very different behavior from smaller particles, as they can see while studying rubber and its properties. They pointed out that these phenomena, which were also manifested in some materials such as gelatin or cotton, made scientists at the time believe that these types of materials were composed of aggregates of small molecular units, linked by

intermolecular forces. Although this erroneous thinking lingered for several years, the definition that persists to this day is the definition given to it by the German chemist and Nobel Prize winner in Chemistry, Hermann Staudinger [1].

The twenty-first century the current definition of these structures as macromolecular substances bound by covalent bonds was formulated in 1920 by Staudinge. The development of the so-called "polymer chemistry" began and since then has only captured the attention of researchers all over the world. Nowadays, polymeric macromolecules are being studied in different scientific fields, such as polymer science or biophysics, where materials resulting from linking monomers through covalent bonds are investigated in different ways and purposes[4].

In general, most polymers were only used to make low-cost items that were only used for a few jobs. And due to the rapid technological progress, it was necessary to replace some industrial materials with newer materials or to reinforce and strengthen the base material with fillers added to the base material to obtain superior specifications [5].

1.2 Polymer Structure

Polymers are large organic molecules (macromolecules) composed of small structural components (monomers) linked together in a polymerization process. Each molecule is made up of thousands of atoms that are connected by covalent chemical bonds, and molecules in polymers are attracted to one another by forces that vary depending on the polymer type [6].

Polymerization is the method of creating synthetic polymers by combining smaller molecules, called monomers, into a chain held together by covalent bonds. The process causes the molecules to bond in a linear, branched, or

network structure, resulting in polymers [7]. These chains of monomers are also called macromolecule. As in the figure (1.1) show polymerization reaction, a large number of monomers become connected by covalent bonds to form a single long molecule [8].

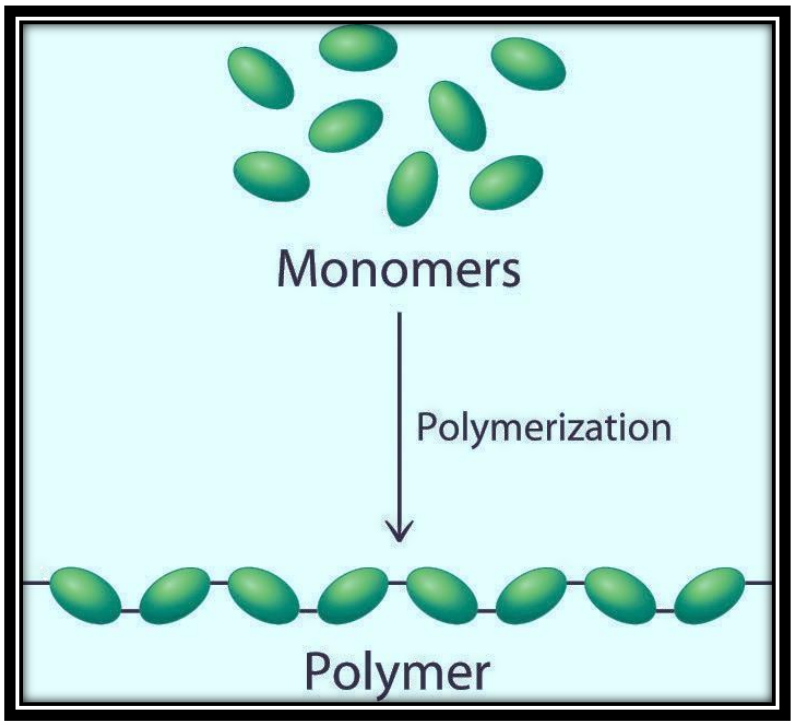

Figure (1.1) : show polymerization reaction[8].

1.3 Classification of Polymers

1.3.1 Thermal classification of polymers

Polymers are classified according to the effect of temperature into:

a. Thermoplastic polymers:

The properties of these polymers are changed by the effect of temperature. When the temperature increases, they become flexible and sticky. By lowering temperature, these polymers return to their original solid state because the molecules in a thermoplastic polymer are connected by relatively weak intermolecular forces (Vander Vales forces). When heated, these molecules can

slide over each other as in polystyrene, polyethylene, polypropylene and polyvinyl chloride [9].

b. Thermoset Polymers:

These polymers are chemically changed when heated. Thermosets are usually three-dimensional networked polymers in which there is a high degree of cross-linking between polymer chains. After being heated, these polymers become insoluble, non-conductive of heat and electricity and hard because molecules of these polymers are connected by strong covalent chemical. Phenol formaldehyde resin and urea-formaldehyde resin are examples of this type of polymers [10].

1.3.2 Structural classification of polymers

Polymers are classified according to their structural composition [11], as shown in the figure:

1. Linear polymers: Van der Waals bonding between chains. Examples: polyethylene and nylon.
2. Branched polymers: chain packing efficiency is reduced compared to linear polymers - lower density.
3. Cross-linked polymers: chain is connected by covalent bonds. Often, it is achieved by adding atoms or molecules that form covalent links between chains. Many rubbers have this structure.
4. Network polymers: 3D networks made from trifunctional mers. Examples: epoxies and phenol-formaldehyde [11].

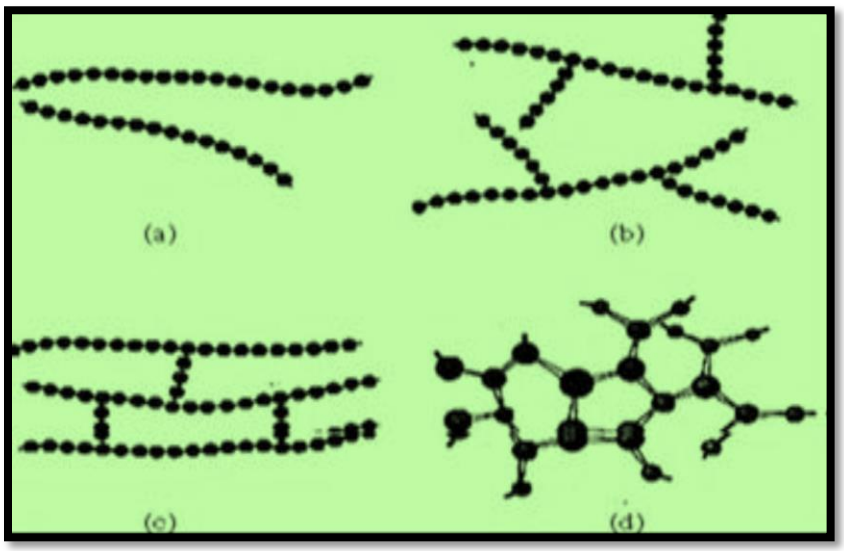

Figure (1.2): Polymer Chains (a) Linear polymers (b) Branched polymers (c) Cross-linked (d) Network polymers [11].

1.3.3 Polymers dependent on homogeneity

Polymers are classified depending on the homogeneity of repeating units into:

a. Homo polymers:

Where the building blocks of a polymer are of one type in poly therphethals ethylene [12].

b. Copolymers:

Where the building blocks of a polymer are more than one type, as in the polymer styrene – butadiene [13].

c. Composite Polymers:

It is the process of adding some material to homogeneous polymers in order to change in some of its characteristics and the entering of new recipes on it [14].

1.4 Polymer Blends

A polymer blend is a mixture of two or more polymers that have been blended together to create a new material with different physical properties. Generally, there are five main types of polymer blend: thermoplastic–thermoplastic

blends, thermoplastic–rubber blends, thermoplastic–thermosetting blends, rubber–thermosetting blends, and polymer–filler blends. Polymer blending has attracted much attention as an easy and cost-effective method of developing polymeric materials that have versatility for commercial applications. In other words, the properties of the blends can be manipulated according to their end use by correct selection of the component polymers [15].

1.5 Biopolymer

Biopolymers are renewable, environmentally friendly and biodegradable materials, which can be used as an ideal substitute for petroleum-based polymers that are synthetic in nature. However, their impact strength, tensile strength, permeability, and thermal stability are relatively low [16]. Hence, the best approach to improve the properties and commercial importance of biopolymers is to incorporate reinforcement material within the micro or nanoregime [17]. The resulting materials are called as environment-friendly polymer composites or biopolymer composites. These composites have a diverse range of next-generation applications in medicine, electronics, construction, packaging and automotive sectors [18].

1.6 Composite Materials

Composite materials are those in which a second component with quite different qualities is mixed in with the polymer so that both contribute to the product's properties. The added component is thought to reinforce the product by increasing its strength or hardness [19]. Composite materials originate in a number of shapes and sizes, and they're made in a diversity of ways. Carbon and glass fibers are the greatest common, and they can be mixed with a diversity of polymer matrices. Their high specific strength, low density, stiffness, excellent fatigue endurance, and low thermal coefficient make them ideal for aerospace and military

applications (in the fiber direction), advanced composite materials possess seen increased use in the aerospace, marine, and automobile industries in recent decades [20]. A composite material system is made up of two or more distinct phases that, when combined, provide aggregate qualities that are unique from their component properties. Composites may be quite useful. Polymer nanocomposites have a wide range of uses, including protective coatings and computer chip packing (insulation) their high strength, temperature stability, process ability and chemical resistance. Improvements in mechanical characteristics and thermal stability [21].

The following two levels of classification are often used to classify composite materials [22]:

1- Typically, the initial stage of categorization involves considering the element of the matrix. The primary categories of composite materials are Organic Matrix Composites (OMCs), Metal Matrix Composites (MMCs), and Ceramic Matrix Composites (CMCs). The phrase "organic matrix composite" often encompasses two distinct categories of composites: Polymer Matrix Composites (PMCs) and carbon matrix composites, sometimes known as carbon composites.

2- The second tier of categorization pertains to the type of reinforcement employed in composite materials, namely fiber reinforced composites, laminar composites, and particle composites.

1.7 Materials Used in The Study

1.7.1 Polyvinyl Alcohol (PVA)

Polyvinyl alcohol (PVA) is in the form of white granules [22]. PVA has attractive properties such as the ability to dissolve in water and its resistance to the action of solvents and oils and has an exceptional ability to adhere to cellulosic materials, so it has wide used. High tensile strength and storage capacity, and electrical and optical properties depending on the type of impurities added [23]. It

is a non-toxic, biocompatible synthetic polymer, that has good transparency and high dielectric strength [24]. PVA is a cheap polymer and is eco-friendly having excellent film forming and adhesive properties, good chemical and mechanical stability and high potential for chemical cross-linking [25]. It has a carbon chain backbone with hydroxyl groups attached to methane carbons/these (OH) groups can be a source of hydrogen bonding and hence assist the formation of polymer composite, polyvinyl alcohol semi- amorphous [26].

The degree of polymerization of PVA (of formula $[CH_2CH(OH)]_n$ with « n » is the number of monomers in a macromolecule) is related to the degree of hydrolysis (each monomer contains one OH groupment) and both affect its solubility. It is well known that when the degree of polymerization of PVA increases, its molecular weight increases. It has been shown that, at a given temperature, the solubility of PVA decreases with increasing molecular weight [27]. Figure (1.3) shows the chemical structure of PVA. Table (1-1) explain some physical and chemical properties of PVA [27].

Table (1.1): Physical and Chemical Properties of Polyvinyl Alcohol (PVA) [27].

Property	Description
Appearance	White to an ivory white granular powder
Molecular formula	$(C_2H_4O)_n$
Solution PH	5- 6.5
Density (g/cm^3)	1.3
Refractive index	1.55
Glass transition temperature T_g(^oC)	85
Melting temperature T_m(^oC)	230
Molecular Weight MW (g/mol)	18000

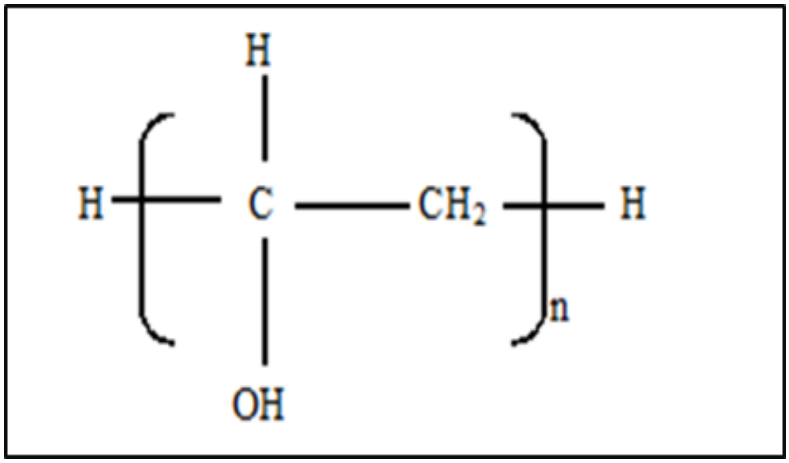

Fig. (1.3): The chemical structure of Polyvinyl alcohol (PVA) [28]

1.7.2 Carboxymethyl Cellulose (CMC)

The most common types of cellulose are the carboxy methyl cellulose (CMC). cellulose is a polymer of linear and large molecular weight, and a plant, renewable, and biodegradable material. although, due to hydrogen bonds that associated with molecular cellulose form does not quickly melt or dissolve in specific solvents. nevertheless, its water-soluble variants find different applications [29]. The aqueous solubility of CMC compared to insoluble cellulose is responsible for the existence of the carboxymethyl groups. CMC is; thus, a low polyaciddissociates to form carboxylate anionic functional groups. The physicochemical properties of polyelectrolytes like CMC in aqueous solution are intimately associated with their conformation. A primary factor affecting the conformation of CMC is the degree of substitution[29].

CMC is used in various products, creams, lotions, and formulation of the toothpaste with which the strong sealing, thickening and stabilizing qualities are included. In fact, because of its polymeric composition, which functions as filmforming agent, it is also used to improve moisturizing effects. among

numerous other applications. CMC is often used for improvement of paper quality, as it inter-bonds between cellulose fibers[30]. The film CMC gel coated on cellulose fibers has enhanced the physical properties of paper for printing purposes. This is used as a drilling material, in addition to large usage of CMC in oil industry. In addition, CMC is applied as a dye thickening in textile industry. CMC as detergent and surfactant are used as anti-dirt agent for protection of fibers surface . CMC has been synthesized from raw cellulose, wood, paper [31]. Cotton-linter fibres, banana trees, Lantana camara, and sugar beet pulp. the principal stage of carboxymethylation is the production of alkali cellulose, which has modified the crystalline structure of cellulose and increased the accessibility of fibers to chemicals by swelling [32]. Table (1.2) explains some properties of CMC [33].

Table (1.2): The Properties of CMC Polymer [33]

Property	Description
Appearance	white to fine powder
Molecular Formula	$C_8H_{16}O_8$
Solution PH	6.5–8.5
Density (g/cm^3)	1.6
Refractive index	1.5-1.7
Glass Transition Temperature T_g (°C)	135
Melting Temperature T_m (°C)	274
Molecular Weight MW (g/mol)	1.7×10^4

1.7.3 Polyvinyl Pyrrolidone (PVP)

Polyvinyl pyrrolidone (PVP), commonly called polyvidone or povidene, is a water soluble polymer and other polar solvents [34]. Polyvinyl pyrrolidone (PVP) is a synthetic polymer, biocompatible, hemocompatible and has been applied as a biomaterial for many years. PVP is remarkable due to its ability to interact with a wide variety of hydrophilic and hydrophobic materials and has properties similar to those of a protein due to its pyrrolidone structure. This material exhibits low immunogenicity, antigenicity and very low toxicity [35]. PVP has the formula $(C_6H_9NO)_n$ [36], as shown in figure (1.4):

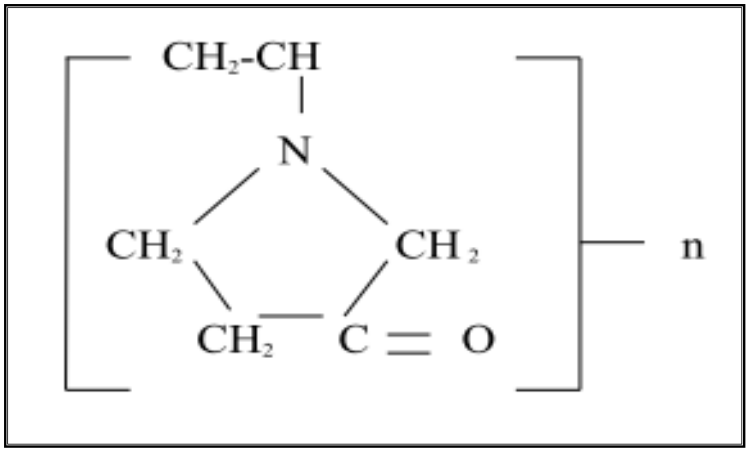

Fig. (1.4):The chemical structure of PVP [37]

PVP is synthesized by polymerization of vinylpyrrolidonein water or isopropanol, and is available in different grades based on molecular weights [38]. Polyvinyl pyrrolidone is a vinyl polymer possessing planar and highly polar side groups dueto the peptide bond in the lactam ring. It deserves a special attention among the conjugated polymers because of the high environmental stability, easy process ability and moderate thermal conductivity [39]. PVP is an amorphous and possesses high glass transition temperature (T_g) (109^{o}C) due to the presence of the

rigid pyrrolidone group, which is known to form various complexes with inorganic salts [40], as shown in table (1.3).

Polyvinyl pyrrolidone has excellent characteristics such as highdielectric constant, dissolubility, stability and compatibility [41]. Polyvinyl pyrrolidonehas good film forming and adhesive behavior on many solid substrates and its formed films exhibits good optical quality (high transmission in visible range), and mechanical strength (easy processing required for application) [42]. PVP is a hydrogel that has been used for a number of biomedical applications. PVP is a branched polymer, more complicated than linear polymer [43,44].

Table (1.3): Physical and chemical properties of polyvinyl pyrrolidone (PVP) [45,46]

Property	Description
Appearance	White to creamy-white
Molecular formula	$(C_6H_9NO)_n$
Density (g/cm^3)	1.25
Solution PH	3-7
Refractive index	1.53
Glass transition temperature T_g (^oC)	109
Melting temperature T_m (°C)	150
Molecular Weight MW (g/mol)	40000

1.7.4 Mg-Chlorophyll Pigments

Chlorophyll pigment photosynthesis is done in green plastics of plant cells, and begins when chlorophyll A and other chromosomes absorb light. Chlorophyll absorbs all visible light colors except green. The colors of the spectrum are absorbed in varying proportions. Chlorophyll absorbs red and violet by a high

proportion, while it absorbs orange, yellow and blue by a low proportion. The absorption of light as such is accompanied by the absorption of the energy deposited in the light, which in turn makes chlorophyll charged with more energy than before the fall of light, and is called in this case "The light is excited and consists of optical particles called photons each containing its energy following the excitement of chlorophyll by electrons that then release the joking electrons from chlorophyll and loaded with high energy. Chlorophyll photosynthesis phases, collectively known as chlorophyll photosynthesis, are defined [47].

The light ionization is that when light induces chlorophyll molecules, electrons acquire high energy that helps them release from chlorophyll making it positive for charge. Some of these high-energy electrons immediately return to chlorophyll and the excess energy soon dissipates in the form of heat or light that generates the fluorescent appearance of chlorophyll [48]. Other electrons are also received by a specialized type of molecule known as electronic vectors found in plastics along with chlorophyll, which carries these electrons from one to the next, accompanied by the gradually excessive energy loss used to build the energy compound (ATP). When the energy level in electrons reaches the same level as that found in chlorophyll before it was aroused by light, it reverts to the chlorophyll that is positive for equation and starts the cycle again [49], and the figure (1.5) shows the types of chlorophyll tinctures [49].

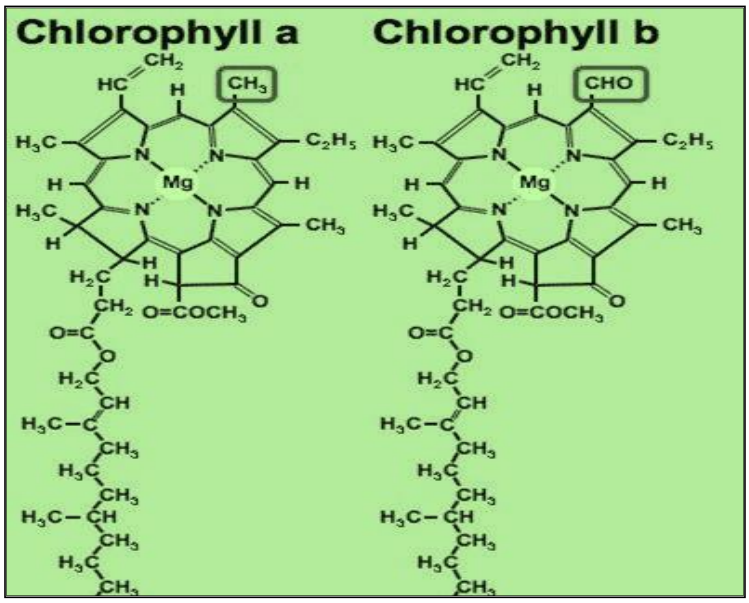

Fig.(1.5): Types of chlorophyll dyes and chemical composition [49].

1.8 Literature Review

El Sayed, *et al.* in (2015) [50] fabricated the (CuO-CMC-PVA) nanocomposite films by using sol-gel process . The results showed that CMC film transparency of increase about (87 %) after PVA addition, but it's decreased with CuO nanoparticles increases. The absorption increased by increase CuO nanoparticles in (CMC-PVA) polymer matrix. The refractive index decreased from (1.645) for CMC to (1.576) for (CMC-PVA) blend, but it increased with increase CuOnanoparticles where the refractive index becomes (1.852). The current–voltage (I–V) features of (CMC-PVA) blend and (CMC-PVA-CuO) nanocomposite films display a non-ohmic behavior. At low temperature the conduction technique of (CMC-PVA) blend is Schottky emission while at high temperatures, the Poole–Frenkel influence area in CuO nanoparticles additive.

Kadhim, *et al.* in (2016) [51] studied some optical properties of (PVA-PEG-PVP) blend by the addition of titanium oxide nanoparticles for biological application. The experimental results show that the absorbance of increases with increasing of the titanium oxide nanoparticles concentration. The energy band gap decreasing and also other optical constants of (PVA-PEG-PVP) blend is increased with the increasing of the titanium oxide nanoparticles concentration.

Bella *et al.* in (2016) [52] fabricated the (PVA-S-CMC) biopolymer blend by using casting method. SEM test showed that (CMC) dispersion thought the (PVA/S) blends and it showed cohesion with the blend. Beside that; the addition of CMC increases the thermal stability of (PVA-S) blend where thermal property of the (PVA-S-CMC) blend improved significantly.

Goswami, *et al.* in (2018) [53] studied the thin films of carboxymethyl cellulose (CMC) and PVA through the process of solution casting. The vanadium pent oxide (V_2O_5) was prepared to yield CMC/PVA-V_2O_5 bio-nanocomposites by in situ precipitation. The AC electrical conductivity was measured within the range of 500–100-1000 Hz. It was found that the conductivity rises along with the rise in frequency at room temperature. T is also responsible for the reduced band gap measured through the UV–VIS spectra. The nanocomposites seem to have strong electrical behavior. Consequently, after the formation of the CMC-PVA-V_2O_5 bio-nanocomposite, the electrical, optical, and mechanical features of CMC films witness a significant improvement. Essentially, this improvement allows the bio-nanocomposites to be applied in various field such as smart windows and storage devices.

Al-Attiyah, *et al*. in (2018) [54] studied the effect of gamma radiation on DC electrical conductivity in (CMC–PVP–PVA–PbO_2) nano-composites. Bio-environmental applications are also used, such as gamma radiation sensor with low cost, low weight and high sensitivity. The structural and electrical properties of these nanocomposites are also studied. The FTIR spectra displays a shift in peak position, as well as a difference in form strength relative pure (CMC–PVP–PVA) films. This suggests a coupling between the respective vibrations of three polymers and lead oxide nanoparticles. It was observed that there is a decrease in transmittance due to a rise in the proportion of lead oxide nano-particles. The electrical properties of this type of nano-composites were measured at room temperature. The findings revealed that the DC conductivity of the (CMC–PVP–PVA) blend rises whenever the rate of PbO_2 nanoparticles increases. The electrical conductivity increases with radiation, induced by the development of polar on species by radiation. The findings of the application revealed that the attenuation coefficients for gamma radiation improved with the rise in nano particles.

Al-Attiyah, *et al.*in (2019) [55] studied the synthesis of novel nano-composites using carboxymethylcellulose (CMC), poly-vinyl pyrrolidone (PVP), and PVA lead oxides nano-particles (CMC–PVP–PVA–PbO_2). They observed the influence of PbO_2nano-particles on the optical characteristics of the (CMC–PVP–PVA) mixture. These nanoparticles were applied to the polymer mixture using weight percentages of (40, 30, and 30) for each of the carboxymethylcellulose, poly-vinyl pyrrolidone, and PVA respectively, with concentrations of 2, 4, 6 and 8 wt%. Considering the optical characteristics of these nanocomposit, the experimental findings indicated an improvement of the absorbance (A), the absorption coefficient the refractive index (n), the extinction coefficient (k), the real and imaginary isolation constants and the optical conductivity of the mixture

(CMC–PVP–PVA) with a rise in wt. percentage of PbO2 NPs. The energy gap of this blend declined with the rise in PbO_2 NP concentration.

Abid, *et al.* in (2020) [56] studied the polymer mixture of PVA-PVP-C.B (Carbon Black) nano-composites. These nano-composites have been prepared and by means of the casting process. The optical properties, FTIR and optical microscope were examined as well. The absorbance of these nanocomposites increased with the rising rates of carbon black nanomaterial concentrations. The energy gap of the nano-composites has decreased with the increase in carbon black (C.B) concentrations. The refractive index, coefficient of absorption, coefficient of extinction, and real and imaginary constants of dielectric of these nano-composites increased along with the increase of carbon black concentrations.

Toman, *et al.* in (2021) [57] prepared (PbO/PVA/PEG) nanocomposites by combining lead oxide weight concentrations (0,1,3,5,7)% wt. The optical microscopy, FTIR and electrical properties of nanocomposites (PVA-CMC/PbO) were studied. The dielectric constant dropped with decreasing dielectric loss, whereas the frequency increased with introducing an electric field. The dielectric loss and constant dielectric of all increased samples with the quantity of lead oxide.

Al-Muntaser, *et al.* in (2022) [58] PVA/CMC-$SrTiO_3$nanocomposites films were prepared using solution casting method. XRD results demonstrate that the crystallinity degree decreases as the content of $SrTiO_3$ NPs increases. The optical properties of PVA/CMC-$SrTiO_3$nanocomposites were enhanced after loading $SrTiO_3$NPs.The relaxation processes and dielectric dispersion of the prepared PNC films were examined and discussed. The findings depicted the applicability and potential uses of these PNC films as advanced optoelectronic applications.

1.9 Aims of the Work

The general objective of this work is:

1. Preparation of chlorophyll to be used as a filler to improve the properties of polymers (CMC-PVA) and (CMC-PVP) blend.
2. Studying some physical properties (morphology, structure, optical) of (CMC-PVA/Mg-Chlorophyll) nanocomposites and CMC-PVP/Mg-Chlorophyll) to know the appropriate application of these films.
3. Applying for the attenuation electromagnetic radiation.

Chapter Two

Theoretical part

2.1 Introduction

This chapter includes a general description of the theoretical part of this study, physical concepts, relationships, scientific clarifications, and laws used to interpret the study results of morphology, structural, Morphology and optical properties used in this work are given by (optical microscopic, scanning electron microscope, Fourier transform infrared spectrometer (FTIR) and X-ray diffraction (XRD), optical properties (the optical constants, fundamental absorption edge, electronic transitions).

2.2 Morphology and Structural Properties

2.2.1 Optical Microscope (OM)

The optical microscope is known to be a compound optical instrument, which makes use of visible light for producing a magnified sample image that is projected on an imaging device or onto the retina of the eye. The term compound refers to the fact that the final image is created through two lenses: the objective lens and the eye-piece or ocular lens, which together perform the magnification of the image [59]. The microscope is most commonly used for minute light-diffracting specimens such as diatoms, bacteria and bacterial flagella, isolated organelles and polymers such as cilia, microtubules, flagella and actin filaments, and silver grains and gold particles in his to chemically labeled cells and tissues. The number of scattering objects in the specimen is an important factor, because the scattering of light from too many objects may brighten the background and obscure fine [60], as shown in figure (2.1).

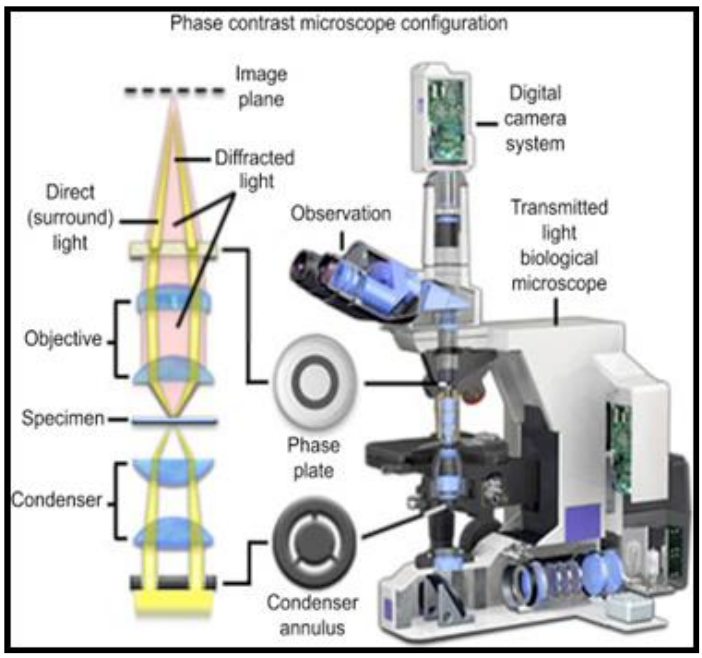

Fig. (2.1): Optical Microscope [60]

2.2.2 Field Emission Scanning Electron Microscope (FESEM)

The (FE-SEM) uses a high-energy beam of electrons to raster scan across a sample surface. Surface topography, composition, as well as other qualities such as electrical conductivity, may be gleaned from signals generated by electrons interacting with atoms in the sample. There are two classes of emission source: thermionic emitter and field emitter [64]. The primary distinction between a SEM and a Field Emission Scanning Electron Microscope (FESEM) is the kind of emitter used (FE-SEM). Tungsten (W) and Lanthanum hexaboride (LaB6) are the most often utilized filament materials in Thermionic Emitters (TEs). When the filament material's work function is exceeded, electrons are released from the filament. Thermionic sources operate with a low level of brightness, cathode material evaporation, and thermal drift. By utilizing Field Emission, you may avoid these problems[65]. The filament is not heated by a Field Emission Source (FE-SEM), also known as a cold cathode field emitter. When the filament is placed

in a massive electrical potential gradient , the emission occurs. Tungsten (W) wire is often used to make the FES, which is then shaped into a sharp point. With developments in secondary electron detector technology, the FE source is compatible with scanning electron microscopes (SEMs) [66]. Cathode and anode voltages are typically between 0.5 to 30 kV, and the microscope needs an extreme vacuum (10–6 Pa) in the column of the microscope, as seen in figure (2.2)[67].

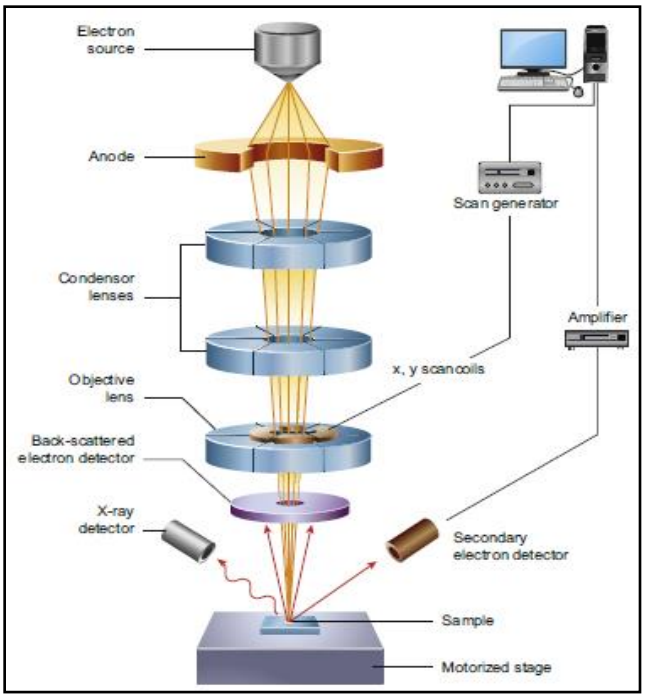

Fig.(2.2): Schematic diagram of the field scanning emission electron microscopy[67].

2.2.3 Fourier Transform Infrared (FTIR) Spectroscopy

Fourier Transforms Infrared (FTIR) is chemical investigative spectroscopy. This measures the infrared intensity with light wave number. The wave numbers consist of infrared light that is divided into three regions, far-infrared, mid-infrared and near-infrared, which are between (4 ~ 400) cm^{-1}, between (400 ~ 4,000) cm^{-1} and finally, between (4,000 ~ 14,000) cm^{-1}, respectively. Infrared radiation is

permitted to pass through a material in FTIR spectroscopy. Some of the infrared radiation is transmitted and some is absorbed by the sample[68].

The resulting spectrum is similar to the sample's molecular fingerprint and contains information about the various chemical groups and chemical bonds present in the sample. Two molecular structures never generate the same infrared spectrum like fingerprints are unique for every person [69].

2.2.4 X-Ray Diffraction (XRD)

X-ray diffraction (XRD) is a powerful instrument for researching electrode materials, particularly cathode materials, to confirm the crystallographic structure, the size of crystallites, and the desired specimen orientation [70]. X-ray radiation is produced by a high-energy electron beam when anode materials such as copper are irradiated [71]. The wavelength range is 0.01-10 nm, and the order of planar crystals in the atom spacing (d) equals the number of atom arrays in the wavelength range [72]. After the dispersion patterns of the material have been analysed, X-rays that can be naturally dispersed from each collection of crystal lattice planes at a specific angle may be utilized to validate the crystal structure after it has been determined what the structure of the crystal is [73]. Bragg's law (equation 2.1) is widely applied to illustrate circumstances of diffraction from planes with spacing (d) [74].

$$n\lambda = 2d\sin\theta \qquad (2.1)$$

In such case, n indicates An number that describes the degree of diffraction, where represents the wavelength of the X-ray beam incident on the crystal lattice, d denotes the spacing of the crystal lattice and denotes the angle of the incident X-ray beam [75]. Figure (2.1) demonstrates that the (XRD) meets Bragg's requirement [76].

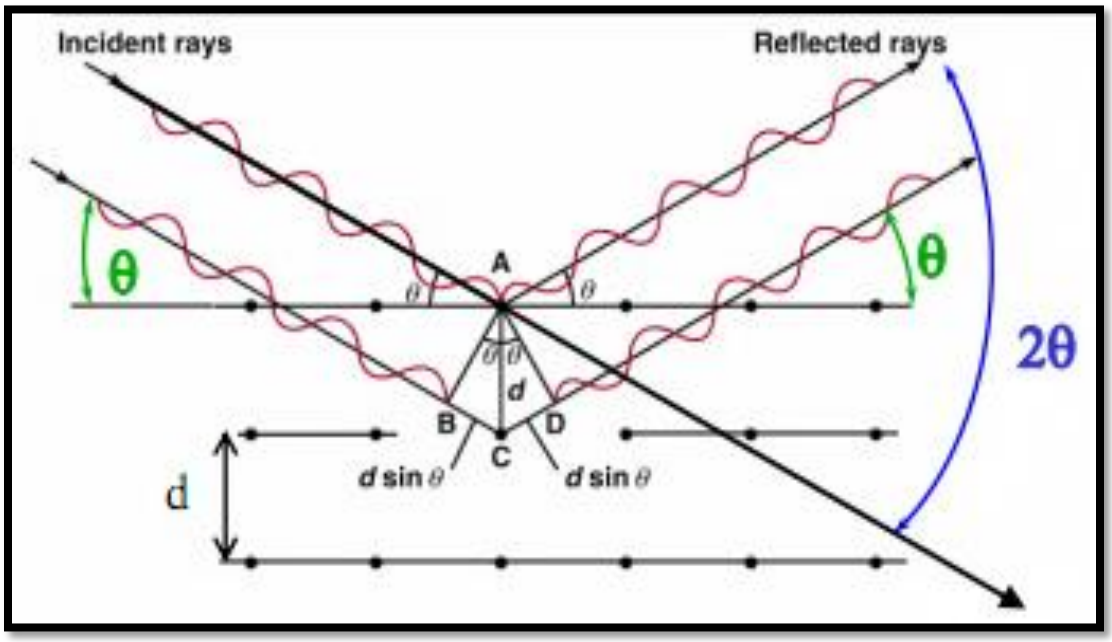

Fig. (2.3) Bragg's Diffraction [76].

In the meanwhile, the Scherrer formula employed to determine the size of the crystallites (D) [77]:

$$D = K\lambda / \beta cos\,(\theta) \qquad \textbf{(2.2)}$$

Where k is the shape factor (0.9), λ is the X-ray wavelength (Å), θ is Bragg diffraction angle of the XRD peak (degree) and β is the full width at the half of the maximum intensity (FWHM)(radian).

2.3 Optical Properties

The purpose of studying the optical properties of polymeric materials is to gain a better knowledge of the internal structure of the polymer and the nature of its bonds, in addition to broadening the scope of potential applications [78].

Knowing the spectrums of absorption and transmittance a polymer assist in identifying many optical properties in different ranges of wavelengths. Examining the ultraviolet spectrum enables us to determine the type of bonds, orbital and

energy beams. The visible spectrum gives sufficient information about a substance's behavior for solar applications. The infrared range is essential for understanding the general structure of a polymer and the constituents that make up its chemical structure [79].

Optical properties represent one of the main factors in its results, which were based on a lot of analyzes about the nature of the atomic structure of the material or to the effect of the absorption material for photons of light in the incidence of the transfer of electronic within the installation packs. This shows the installation of power packs as well as the energy gap whether directly or indirectly. That is provided with information about the nature of the change constants visual such as, absorption coefficient, coefficient of refraction, extinction coefficient and others [80].

2.3.1 Absorbance(A)

Absorbance is defined as the ratio of the intensity of the absorbed light (I_A) to the incident intensity of light (I_o), which is given in the following equation [81]:

$$A=I_A/I_o \qquad (2.3)$$

Where: I_A intensity of the absorbed light and I_o incident intensity of light [82].

2.3.2 Absorption Coefficient (*α*)

The absorption coefficient is defined as a percentage decrease in the energy flux of the incident rays concerning the unit distance in the direction of propagation of the incident wave.

The relationship between incident (I_o) and penetrating (I) is defined in the following equation as being related to the absorption of light [83]:

$$I = I_\circ e^{-\alpha t} \qquad (2.4)$$

where (t) is the thickness of the matter and (α) is the absorption coefficient, it is measured by cm^{-1}[84].

$$\alpha t = 2.303 \log I/I_\circ \qquad (2.5)$$

where log I/I_o is the absorbing number (A). This is the way to measure the absorption coefficient [84]:

$$\alpha = (2.303)A/t \qquad (2.6)$$

Where: t is the sample thickness in cm, A is the absorption of the material [84].

2.3.3 Fundamental Absorption Edge

The quick increase in absorbency when the absorbed energy radiation nearly equals the energy band gap is known as the fundamental absorption edge. As a result, the basic absorption edge represents a smaller energy difference between the valance band's peaks (V.B) and the conduction band's bottom point (C.B). As shown in Figure (2.4), the absorption regions can be divided into three categories [85].

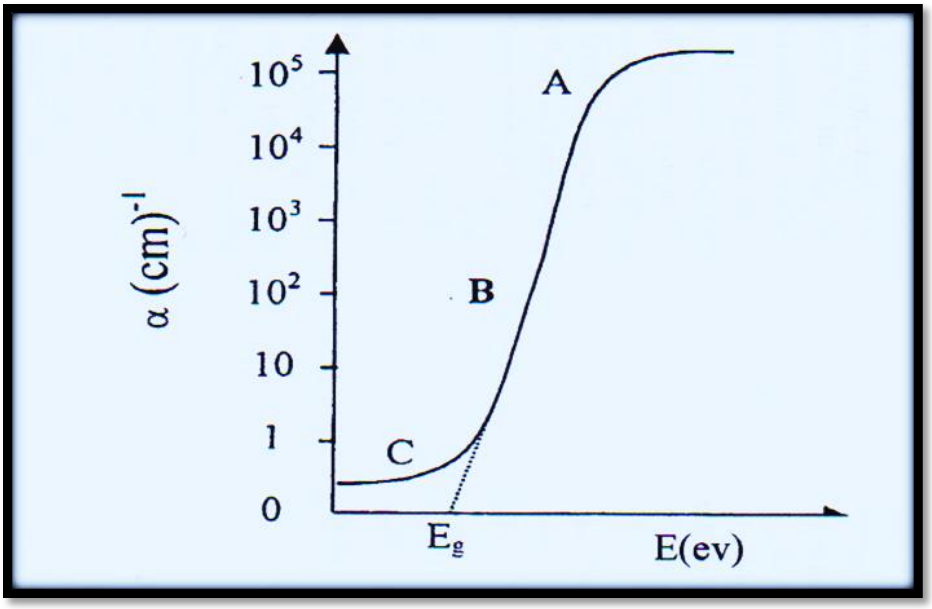

Fig (2.4): The variation of absorption edge with absorption regions [83].

A) High absorption region: In component A, the value of (α) is larger than or equal to $10^4 cm^{-1}$. This region could be used to calculate the size of the forbidden optical band gap (E_{gopt}) [86].

B) Exponential region: The value of (α) in component B should be between 1 cm^{-1} and $10^4 cm^{-1}$. It shows the transition from the extended level at the top of the valence band to the localized level at the conductive band, and vice versa, from the local level at the bottom of the conductive band to the extended level at the top [88].

C) Low absorption region: Part C involves a relatively smaller value of (α), being about $\alpha<1 cm^{-1}$. In this location, the transition happens as a result of the state of density within caused by structural flaws [89].

2.3.4 Transmittance (T)

The transmittance (T) is the ratio of the intensity of transmitted rays from the film (I_T) to the intensity of incident rays on the film (I_o) and can be calculated as follows [90]:

$$T = \frac{I_T}{I_o} \qquad (2.7)$$

Where : I_T intensity of transmitted rays from the film and I_o the intensity of incident rays on the film[90].

2.3.5 The Electronic Transitions

Electronic transition can be divided into two types: direct and indirect.

2.3.5.1 Direct Transitions

This kind of transitions occurs in semi-conductors, where the bottom of the conduction is precisely above the top of the valance band, thus implying that they share similar wave vector values i.e. ($\Delta K=0$). In such a case, the absorption would occur at ($h\upsilon = E_g^{opt}$). As a result, phonons do not participate in direct transition since their wave vector (K) is substantially larger than that of photons[91]. This transition type necessitates the use of momentum and energy conservation principles. The condition for conserving the wave vector is not satisfied by the direct photon transition to the energy of the least gap, because photon wave vectors could be ignored in the provided energy range. Direct transitions are divided into two types [92].

a) Direct allowed transition

It occurs between the top and bottom points of the valance band and, between the top and bottom points of the conduction transition[92]. as shown, in Figure (2.5-a).

b) Direct forbidden transitions

It occurs between the valance band's close top points and the conductive band's bottom points, as shown, in Figure (2.5-b). The absorption coefficient for this transition type is given by [92]:

$$\alpha h\upsilon = B\,(h\upsilon - E_g^{opt})^r \qquad (2.\ 8)$$

Where (E_g^{opt}) is the energy gap between direct transition

B : the constant (according to the type of material)

r : the exponential constant, its value depended on type of transition.

r =1/2 for the allowed direct transition.

r =3/2 for the forbidden direct transition.

2.3.5.2. Indirect Transitions

In these transitions type, the bottom of conductive band is not over the top of valance band. The electron transits from valance band to conductive band perpendicularly where the value of the wave vector of electron before and after transition is not equal ($\Delta K \neq 0$). This transition type happens with the help of particle called "Phonon", for conservation of the energy and momentum law. There are two types of indirect transitions [93], they are:

c) Allowed Indirect Transitions : These transitions happen between the top of valance band and the bottom of conductive band which is found in the difference region of (K-space), as in Figure (2.5-c).

d) Forbidden Indirect Transitions : These transitions happen between near points in the top of valance band and near points in the bottom of conductive band , as shown in Figure (2.5-d).

The absorption coefficient for transition with a phonon absorption is given by [93]:

$$\alpha h\nu = B(h\nu - E_g^{opt.} \pm E_{ph.})^r \qquad (2.\ 9)$$

Where: E_{ph} energy of phonon, is (-) when phonon absorption, and (+) when phonon emission.

r = 2 for the allowed indirect transition, r = 3 for the forbidden indirect transition.

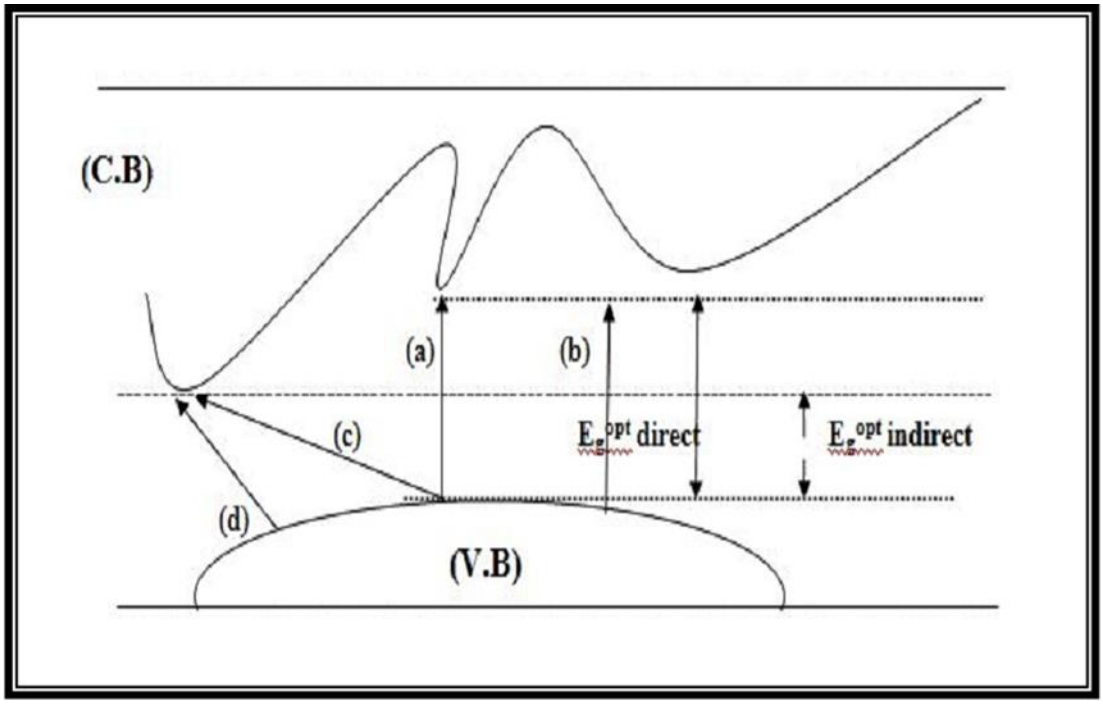

Figure (2.5): The Electronic Transitions Types of (a) Allowed direct, (b) Forbidden Direct Transition, (c) Allowed Indirect and (d) Forbidden Indirect Transitions [92].

2.3.6 The Refractive Index (n)

Ratio of vacuum low velocity with light velocity within the material can be described as refractive index. The refractive index value (n) was determined using equation (2.8), depending on the reflection and extinguishing coefficient (K_0) [94] :

$$R = \frac{(n-1)^2+K_0^2}{(n+1)^2+K_0^2} \qquad (2.10)$$

where (K_o) is the Extinction coefficient. Reflectivity can be obtained from absorption and transmission spectrum in accordance to the law of conservation of energy by the relation [94].

$$R + A + T=1 \qquad (2.11)$$

where: R:is the reflectivity, T:is the transmittance, A: is the absorption The following equation can be used to express refractive index [94]:

$$n = (1 + R^{\frac{1}{2}})/(1 - R^{\frac{1}{2}}) \qquad (2.12)$$

2.3.7 The Extinction Coefficient (K_o)

The amount of attenuation of an electro-magnetic pulse passing through a substance is represented by the extinction coefficient (K_o). The density of free electrons within the material and its structure determines its value. The imaginary portion of the complex refractive index (n) is this:

$$N = n - i K_o \qquad (2.13)$$

Where (n) represents the real part of refractive index. N : complex refractive index which depends on the material type, crystal structure (grain size), crystal defects, stress in crystal, extinction coefficient (K_o) , is given by following equation:

$$K_o = \alpha \lambda/4\pi \qquad (2.14)$$

Where (K_o) is the extinction coefficient, and (λ) is the wavelength of incident light [95].

2.3.8 The Dielectric Constant (ε)

The Dielectric Constant represents the ability of a matter for polarization, the matter can respond to different frequencies in a complex manner, at optical frequencies represented by light waves the electronic polarity is dominating above other remaining types of polarization. The real and imaginary dielectric constant can be calculated by the following equation [96] :

$$\varepsilon = \varepsilon_1 - i\varepsilon_2 \qquad (2.15)$$

where: ε is the complex dielectric constant and (ε_1, $i\varepsilon_2$) are the real and the imaginary parts of the dielectric constant, respectively.

where: ε is the complex dielectric constant and (ε_1, $i\varepsilon_2$) are the imaginary and real parts of the dielectric constant, respectively. The dielectric constant's real and imaginary components are connected to and values[97].

$$\varepsilon = N^2 \qquad (2.16)$$

$$(n - ik_o)^2 = \varepsilon_1 - i\varepsilon_2 \qquad (2.17)$$

From equation (2.13) real and imaginary complex dielectric coefficient can be written as follows :

$$\varepsilon_1 = (n^2 - k_o^2) \qquad (2.18)$$

$$\varepsilon_2 = (2nk_o) \qquad (2.19)$$

2.3.9 The Optical Conductivity (σ_{op})

The optical conductivity (**σ_{op}**) relies directly on the absorption coefficient (α) and refractive index (n), using the following relation [98]:

$$\sigma_{op} = \frac{\alpha n c}{4\pi} \qquad (2.\ 20)$$

where c is the velocity of light, α is the absorption coefficient .

Chapter Three

Experimental Part

3.1 Introduction

This chapter includes an explanation of the mechanism of how to prepare chlorophyll from a natural and familiar substance in our daily life, with several experimental steps. It also includes the stages of preparing (CMC/PVA/Mg-Chlorophyll) and (CMC/PVP/Mg-Chlorophyll) nanocomposite samples tests and measurement steps such as: Optical Microscopic (OM), Scanning Electron Microscope (FESEM), Fourier Transformation Infrared Radiation (FTIR), X-Ray Diffraction (XRD) and optical measurements.

3.2 Materials used in this Investigation

3.2.1 Polyvinyl alcohol (PVA):

used as powder form and could be obtained from Panveac Spain company with high purity (99.8%).

3.2.2 Polyvinyl Pyrrolidone (PVP):

used as powder form and could be obtained from Panveac Spain company white with high purity (99.8%).

3.2.3 Carboxymethyl Cellulose (CMC):

It was obtained as powder form and could be obtained from Panveac Spain company with high purity (99.8%).

3.3 The Additive Material

3.3.1 Filler material (Mg chlorophyll):

It is added to the polymer mixture as a filler with nano-diameters, It was extracted from celery.

3.4 Preparation of Mg Chlorophyll and (CMC/PVA/Mg-Chlorophyll) and (CMC/PVP/Mg-Chlorophyll) nanocomposite.

Chlorophyll was prepared from the celery plant, where the celery leaves were cleaned (washed) and then dried at a temperature of 40C by microwave. Acetone was added to the dried celery leaves, mixed and then kneaded homogeneously and left to dry

at room temperature. After drying, the mixture was filtered by A piece of cloth that is semi-permeable to separate the fine substance, which is chlorophyll, and thus we will get chlorophyll in the form of a powder, and it will be kept inside a tight glass contained.

The materials used in this paper are (CMC), (PVA) and (Mg-Chlorophyll). The nanocomposite was prepared by dissolving 0.5 g from CMC in 50 mL of distilled water for 30 minutes under continuous stirring using a magnetic stirrer at 80 °C to achieve a more homogeneous solution and then added 0.5 g from PVA with continuous stirring and temperature 40°C until become homogenous. To investigate the nanocomposite, Mg-Chlorophyll were added to the blend (CMC/PVA) in various ratio (0,2,4 and 6) wt. % as shown in Figure (3.1).

At the same procedure above, the (CMC/PVP) was prepared and added Mg-Chlorophyll to the blend (CMC/PVP) in various ratio (0,2,4 and 6) wt. % as shown in Figure (3.2).

Table (3-1) PVA, CMC and Mg-Chlorophyll with different content

Concentration **wt%**		
CMC	**PVA**	**Mg-Chlorophyll**
50	50	0
49	49	2
48	48	4
47	47	6
46	46	8

Table (3-2) PVP, CMC and Mg-Chlorophyll with different content

Concentration wt%		
CMC	PVP	Mg-Chlorophyll
50	50	0
49	49	2
48	48	4
47	47	6
46	46	8

To make composite films, a casting process was used. Pour each weight percentage into a plastic Petri dish and allow drying at room temperature for 7-10 days. Then are taken measurements structural and optical properties.

3.5 Measurements of Structural Properties

3.5.1 Microscopic Examination (OM)

The (CMC/PVA/Mg-Chlorophyll) and (CMC/PVP/Mg-Chlorophyll) nanocomposite, were examined by an optical microscope by the Olympus name (Top View) type (Nikon-73346), and fitted with an automatic camera operated by light intensity under magnification (10x). This measurement was carried out for at the University of Babylon/ College of Education for Pure Sciences/ Department of Physics.

3.5.2 Field Emission Scanning Electron Microscope (FESEM).

Via high–resolution photographs and magnification, describe the essence and morphology of the prepared films' surface, as well as the internal structure of the films' substance. Photons with X-ray wavelengths are produced when primary electron's reaction with the sample. The atomic ratio in the sample can be

measured using energy dispersive spectroscopy after this emission is detected by (ΣIGMA, JSM-7610F, Carl Zeiss, Germany) image operating at an accelerating voltage of 10 kV. The element ratio and surface morphology of the film that were produced were examined utilizing FE-SEM.

3.5.3 X-Ray Diffraction (XRD)

The main aim of these measurements is to study the form of structure of the prepared films. Determining the general structure of bulk solids, including lattice constants, identifying unknown materials, orienting single crystals, orienting polycrystalles, flaws and stresses. has long been used in this experimental technique.

"X-ray diffraction" by the X-ray diffract meter device (^{o}XRD-6) from SHIMADZU, which records a measure of the intensity as a function the angle of Bragg. The system's circumstances were: CuK_{α} emits radiation with a wavelength of 1.5406 nm from a CuK_{α} sourcTarget: Cu current is equal to 30 mA. The voltage is equal to 40 kV. The scanning speed is 0.25 degrees per minute. A total of two "X-ray scans) are" done (between) the two-point values of zero and eighty degrees.

3.5.4 FTIR Spectrometer

The FTIR spectra of (CMC/PVA/Mg-Chlorophyll) and (CMC/PVP/Mg-Chlorophyll) nanocomposite, were acquired by an FTIR in strument (Bruker company, German origin, type vertex -70). FTIR was implemented in University of Babylon/ College of Education for Pure Sciences / Department of Physics. The findings of this investigation show that considered wave number range is (500-4000) $cm^{-.1}$.

3.6 Optical Properties

The optical properties of (CMC/PVA/Mg-Chlorophyll) and (CMC/PVP/Mg-Chlorophyll) nanocomposite double beam spectrophotometer (Shimadzu, UV -

1800A) with a measure nanocomposite in this study (190-1100) nm. The Department of Physics at the University of Babylon / College of Education for Pure Sciences, at room temperature, the absorption spectra have been measured and analyzed. The absorption coefficient, optical constants, extinction coefficient, refractive index and energy gaps were calculated with the use of a computer software, which may be found here.

Chapter Four

Results, Discussion and Future Works

4.1 Introduction

This chapter emphases on the results and discussion of the X-ray diffraction (XRD) for (CMC/PVA/Mg-Chlorophyll) and (CMC/PVP/Mg-Chlorophyll) nanocomposite and then study the Fourier transform technique (FT-IR), Scanning electron microscopy (FESEM), Optical microscope (OM).

4.2 Structural and Morphological Properties

4.2.1 X-ray Diffraction (XRD)

XRD technique is the most common analysis tool to depict the Mg-Chlorophyll formation and to know the crystal particle size and the crystalline phase present. The XRD patterns for pure CMC/PVA and pure CMC/PVP blend with various content of Mg-Chlorophyll Pigments (2, 4, 6 and 8 wt.%) are shown in Figures (4.1) (4.2) respectively. Peaks of XRD were recorded between 10^{o} - 80^{o}.

From Figure (4.1), the pure CMC/PVA exhibited two diffraction peaks at $2\theta = 21.91°$ corresponding to the typical cellulose II partially crystalline nature and which may be due to the semicrystalline structure of PVA [99,100,101] and low intensity $2\theta = 11.91°$ which related to the structure of PVA [100]. Also from this figure, with added different concentration of Mg-Chlorophyll Pigments (2, 4, 6 and 8 wt.%), the intensity increased and there are no peaks appears, which due to the low concentration added to the PVA/CMC polymer blend and also due to the broad peaks of the PVA/CMC which disappear all peaks.

From Figure (4.2), the XRD patterns of pure CMC/PVP blend for both PVP and CMC polymers confirm their semicrystalline nature. The CMC spectrum shows a broad peak at $2\theta=19.34°$ [102] and PVP film is characterized by peak halos centered at $2\theta= 22.54°$ [103]. The intensity of this peaks increased with

increasing concentration of Mg-Chlorophyll Pigments and there are no peaks appears, which due to the low concentration added to the PVP/CMC polymer blend and also due to the broad peaks of the PVP/CMC which disappear all peaks.

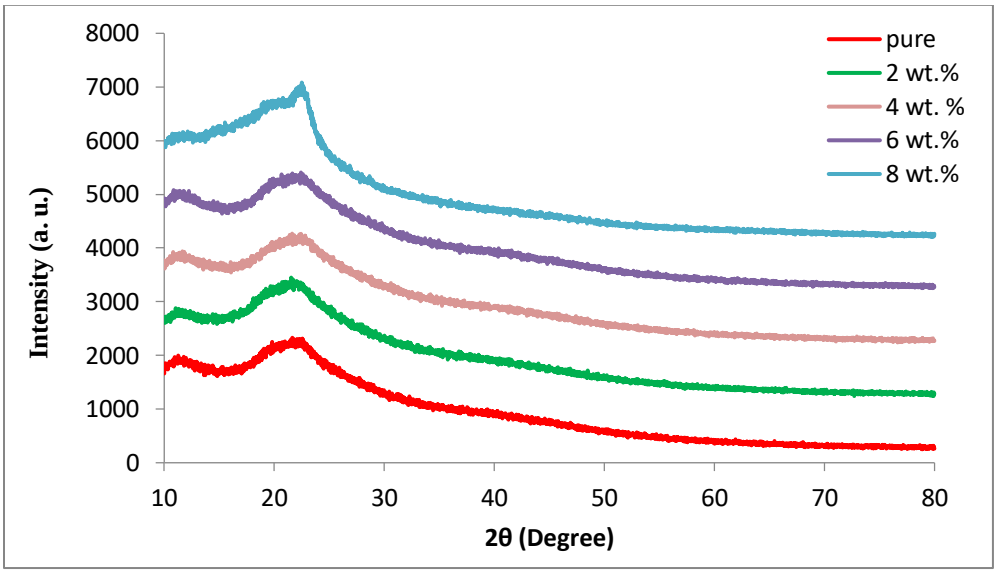

Fig. (4.1): XRD pattern of (CMC/PVA/Mg-Chlorophyll) nanocomposites.

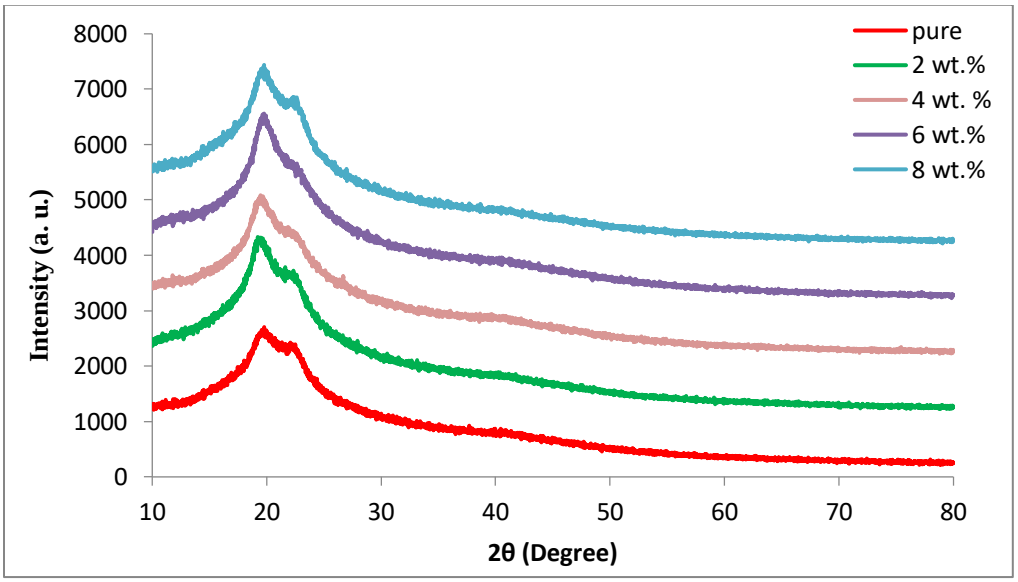

Fig. (4.2): XRD pattern of (CMC/PVP/Mg-Chlorophyll) nanocomposites.

4.2.2 Field Emission Scanning Electron Microscope (FESEM).

To examine the morphological of (CMC/PVA/Mg-Chlorophyll) and (CMC/PVP/Mg-Chlorophyll) nanocomposite using field emission scanning electron microscope (FE-SEM).

Figures (4.3), (4.4) demonstrate the FE-SEM images of pure CMC/PVA, CMC/PVP and (CMC/PVA/Mg-Chlorophyll) and (CMC/PVP/Mg-Chlorophyll) nanocomposites with various concentration (2, 4, 6 and 8 wt.%) of Mg-Chlorophyll respectively with a different magnification and scale.

From the Figure (4.3A), showed homogeneous, grainy, coarse surface shapes and the surface suffers from some cracks and that the polymer crystals, while in Figure (4.4 A) exhibit smooth and homogenous surface, which mean a successful this method to prepare films. On the other hand, Mg-Chlorophyll with concentration 2 wt.% at these figures in the CMC/PVA and CMC/PVA nanocomposite revealed affected the polymer matrix and showed good dispersion and granular structure without assemblies, but the crack still appeared. Increasing the loading ratio of Mg-Chlorophyll from 4 to 8 wt. %, the cracks at the surface were significantly reduced too difficult to recognize and became very smooth compared with other samples. Moreover, Mg-Chlorophyll create network inside the polymer blend. This constitutes paths inside the nanocomposites of charge carriers. This system can allow charge carriers to pass through the paths. This could referee good adhesions and stronger interfacial interaction of the nanocomposite in agreement with FTIR results that showed a change in the functional peaks and XRD results [104].

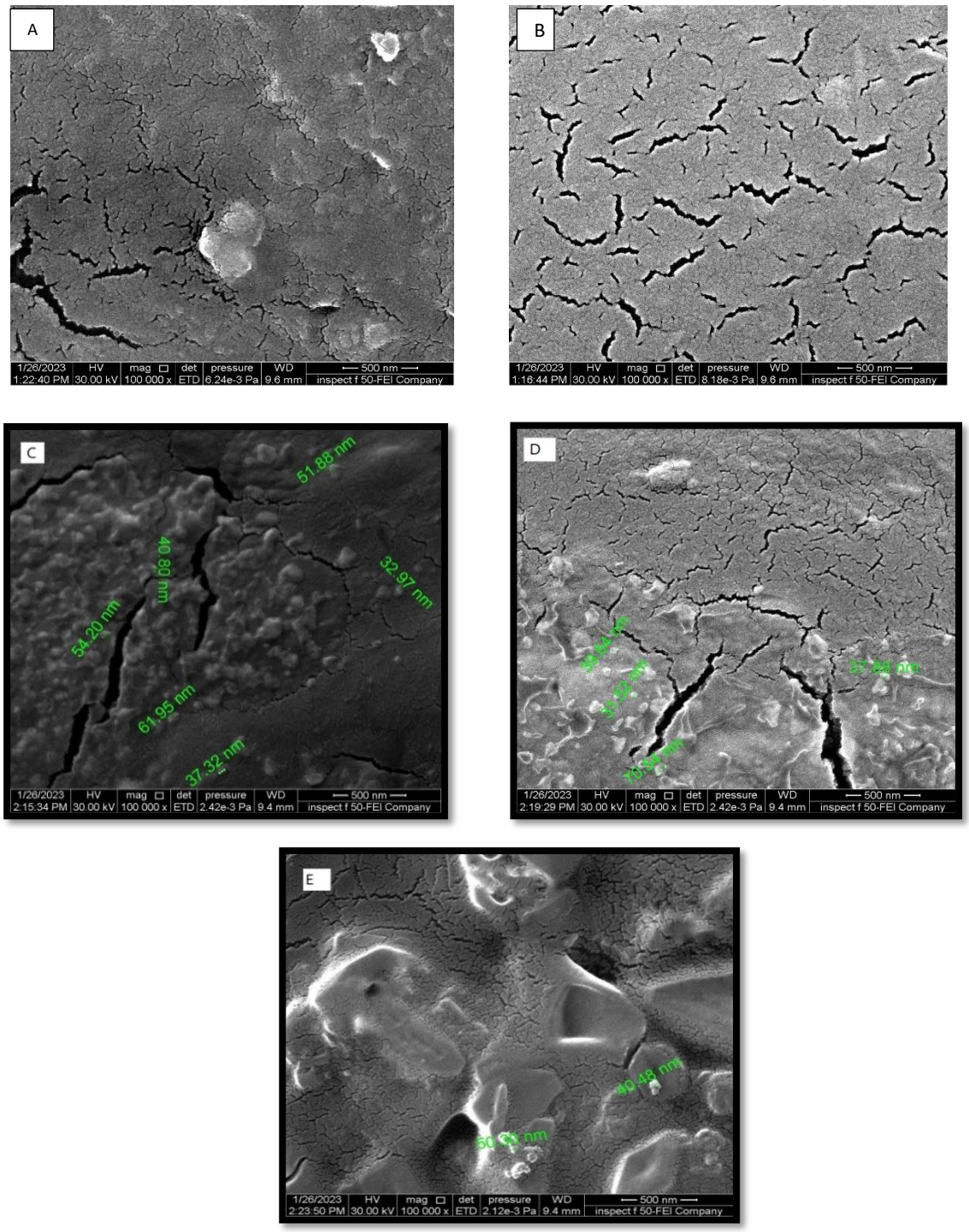

Fig. (4.3) FSEM images of (CMC/PVA/Mg-Chlorophyll) nanocomposites, (A) for (CMC/PVA), (B) 2 wt.% Mg-Chlorophyll, (C) 4 wt.% Mg-Chlorophyll, (D) 6 wt.% Mg-Chlorophyll, (E) 8 wt.% Mg-Chlorophyll

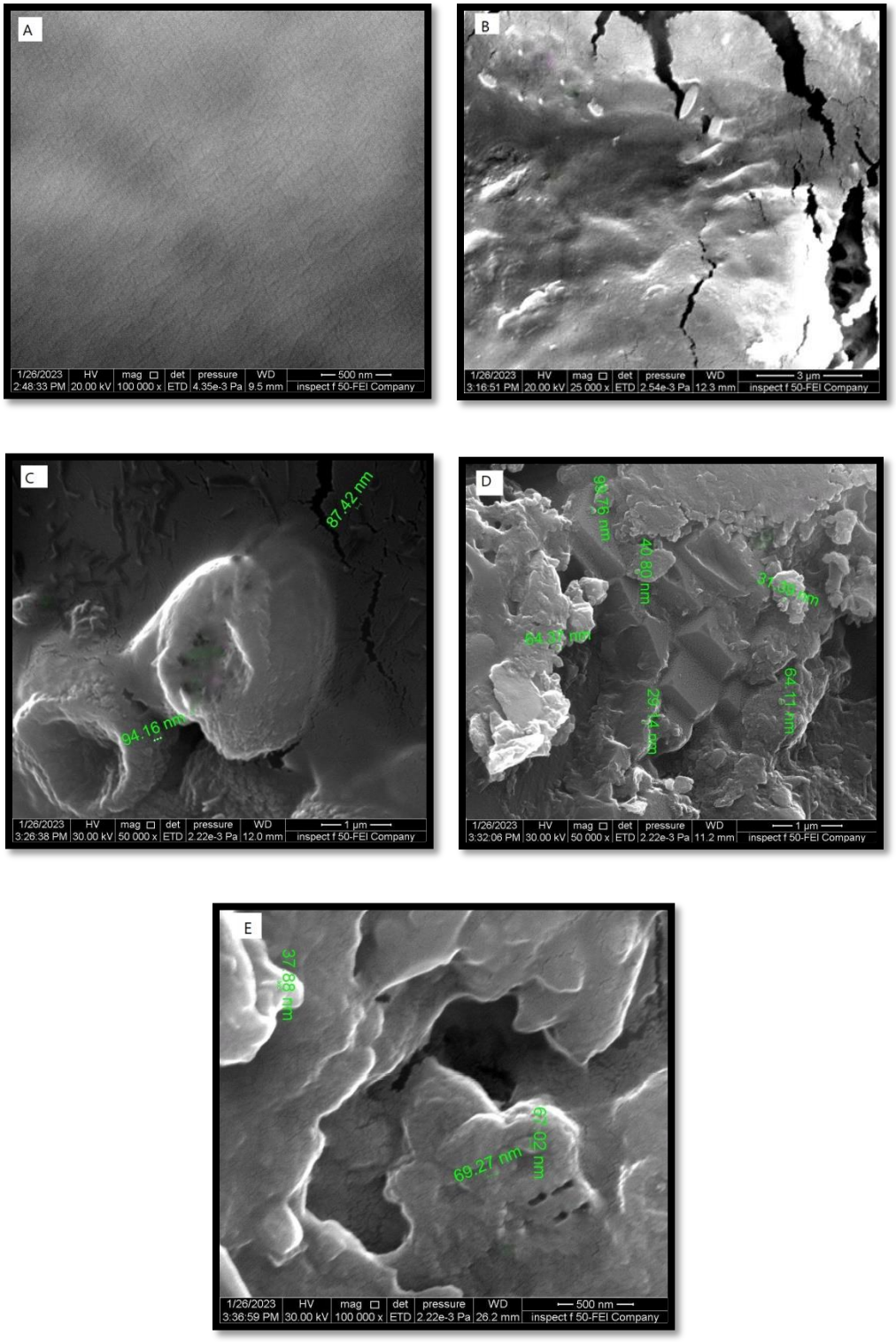

Fig. (4.4) FSEM images of (CMC/PVP/Mg-Chlorophyll) nanocomposites, (A) for (CMC/PVP), (B) 2 wt.% Mg-Chlorophyll, (C) 4 wt.% Mg-Chlorophyll, (D) 6 wt.% Mg-Chlorophyll, (E)

8 wt.% Mg-Chlorophyll.

4.2.3 Optical Microscope.

Figures (4.5) and (4.6) show the optical microscope of (CMC/PVA/Mg-Chlorophyll) and (CMC/PVP/Mg-Chlorophyll) nanocomposites with various content of Mg-Chlorophyll Pigments (2, 4, 6 and 8 wt.%) at magnification power (10x). The optical microscope gives the change of surface morphology of nanocomposites. Compared with pure sample images, there are many differences among this sample and both nanocomposites with adding different concentrations of Mg-Chlorophyll, both figures show the addition of Mg-Chlorophyll distributed through the polymeric blend with homogenous and ordered shape as well as the apparent of Mg-Chlorophyll network inside the polymer blend. This constitutes paths inside the nanocomposites of charge carriers. This system can allow charge carriers to pass through the paths.

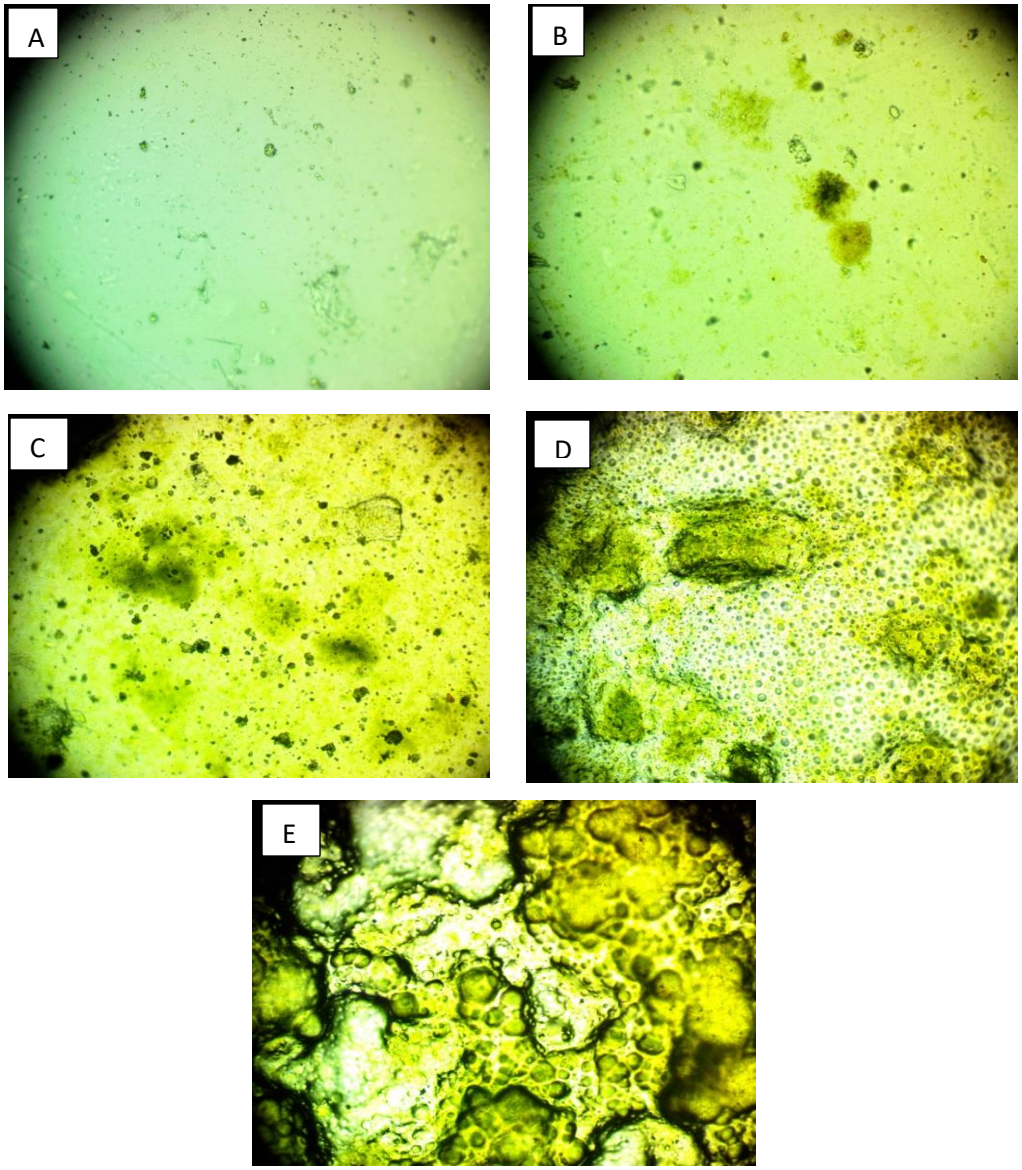

Fig (4.5): Photomicrograph images for (CMC-PVA-Mg-Chlorophyll) nanocomposite: (A) (CMC-PVA) blend, (B) 2wt% Mg-Chlorophyll,(C) 4wt% Mg-Chlorophyll, (D) 6wt% Mg-Chlorophyll and 8wt.%Mg-Chlorophyll

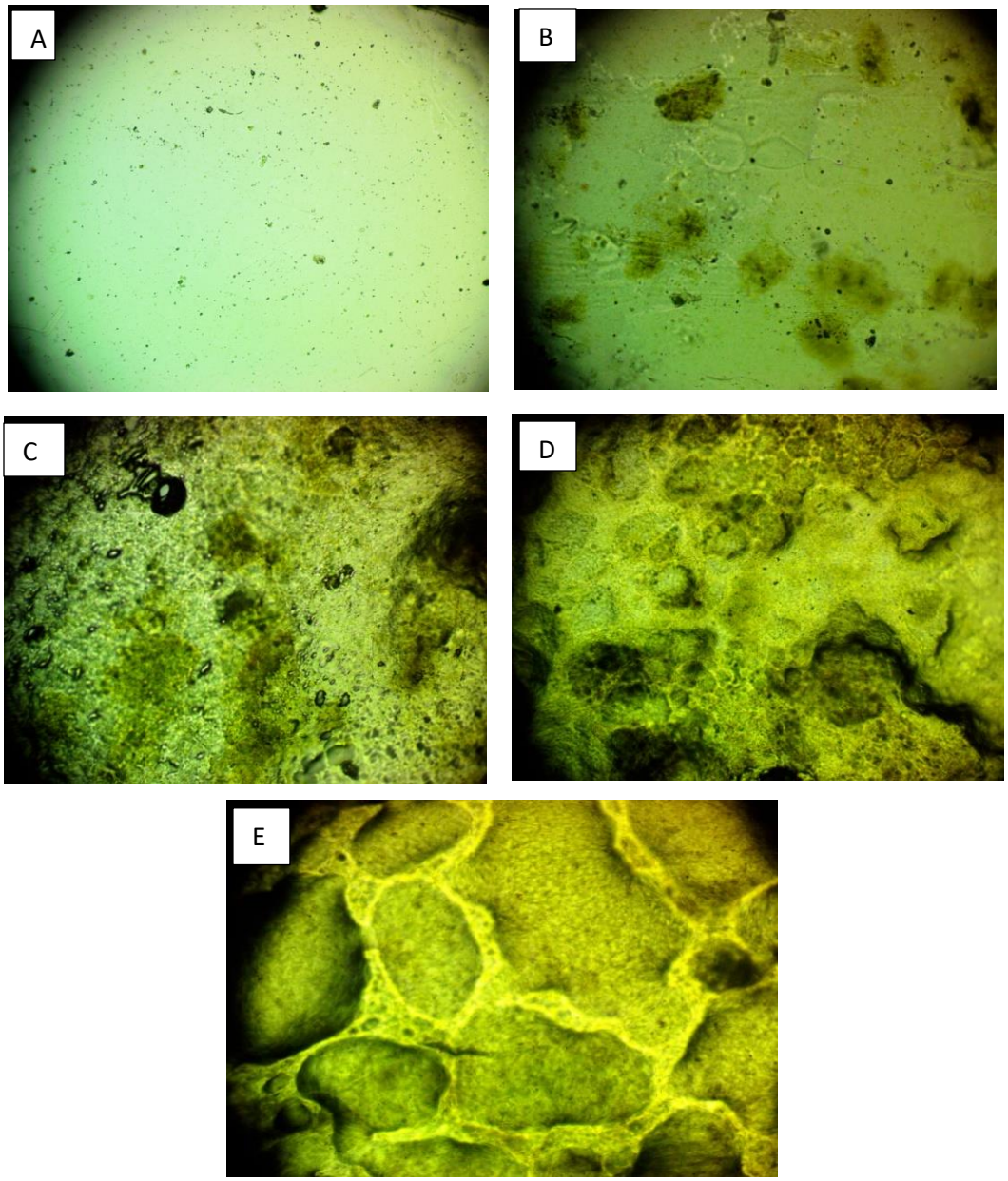

Fig (4.6): Photomicrograph images for (CMC-PVP-Mg-Chlorophyll) nanocomposite: (A) (CMC-PVP) blend, (B) 2wt% Mg-Chlorophyll,(C) 4wt% Mg-Chlorophyll, (D) 6wt% Mg-Chlorophyll and 8wt.%Mg-Chlorophyll

4.2.4 Fourier Transform Infrared Radiation (FTIR) of (CMC/PVA/Mg-Chlorophyll) and (CMC/PVP/ Mg-Chlorophyll) nanocomposites

The FTIR spectra of (CMC/PVA/Mg-Chlorophyll) and (CMC/PVP/ Mg-Chlorophyll) nanocomposites with various content of Mg-Chlorophyll Pigments (2, 4, 6 and 8 wt.%) were recorded at room temperature in the region (500-4000) cm^{-1} as shown in Figures (4.7) and (4.8).

From this Figure (4.7A), Its exhibit eleven major absorption peaks. The broad peak at 3279.59 cm^{-1} assigned to the stretching vibration of the alcohol group (OH) in the polymer matrix chain. The intense peak at 2941 cm^{-1} corresponds to the CH_2 asymmetric stretching. Additionally, the peak at 1732.21 cm^{-1} corresponds to the Stretching C=O and C-O from acetate group remaining from PVA. The peak at 1591.53 attributed to the Carboxylate (COO^-) stretching group, which indicate to the CMC polymer chain and the peaks at 1420 cm^{-1} and 1381 cm^{-1} corresponds to the C–H deformation vibration CH_2 out of plan bending vibration. The peak at 1318 corresponding to the OH bending. Moreover, the peaks 1248.97 cm^{-1} and 1022.35 cm^{-1} corresponding to the CH_2 bending and CH-O-CH_2 stretching respectively, while the peaks 822 cm^{-1} and 615 cm^{-1} attributed to the CH_2 rocking vibration and aromatic ring out of plane bends [105, 106].

The Figure (4.8 A), Its exhibit eight major absorption peaks. The broad peak at 3396.15 cm^{-1} assigned to the OH stretching. The peak at 2992 cm^{-1} corresponds to the CH_2 asymmetric stretching, while the peak 1649.95 cm^{-1} assigned to the symmetric and asymmetric of C=O. Additionally, the peak at 1422.53 cm^{-1} corresponds to the CH_2 scissoring. The peak at 1289.15 attributed to the CH_2 (wagging or twisting) or N–OH complex and the peaks at 1018.53 cm^{-1} and 615 cm^{-1} corresponds to the CH_2–O–CH_2 stretching and C–N bending [107, 108].

As was mentioned, the intensity of these bands decreased and slightly shifted toward higher wavenumbers, which is a sign that hydrogen bonds were formed by the physical contact between the functional groups in the polymer blend and both Mg-Chlorophyll Pigments. The results agree with the results of the previous researchers [56].

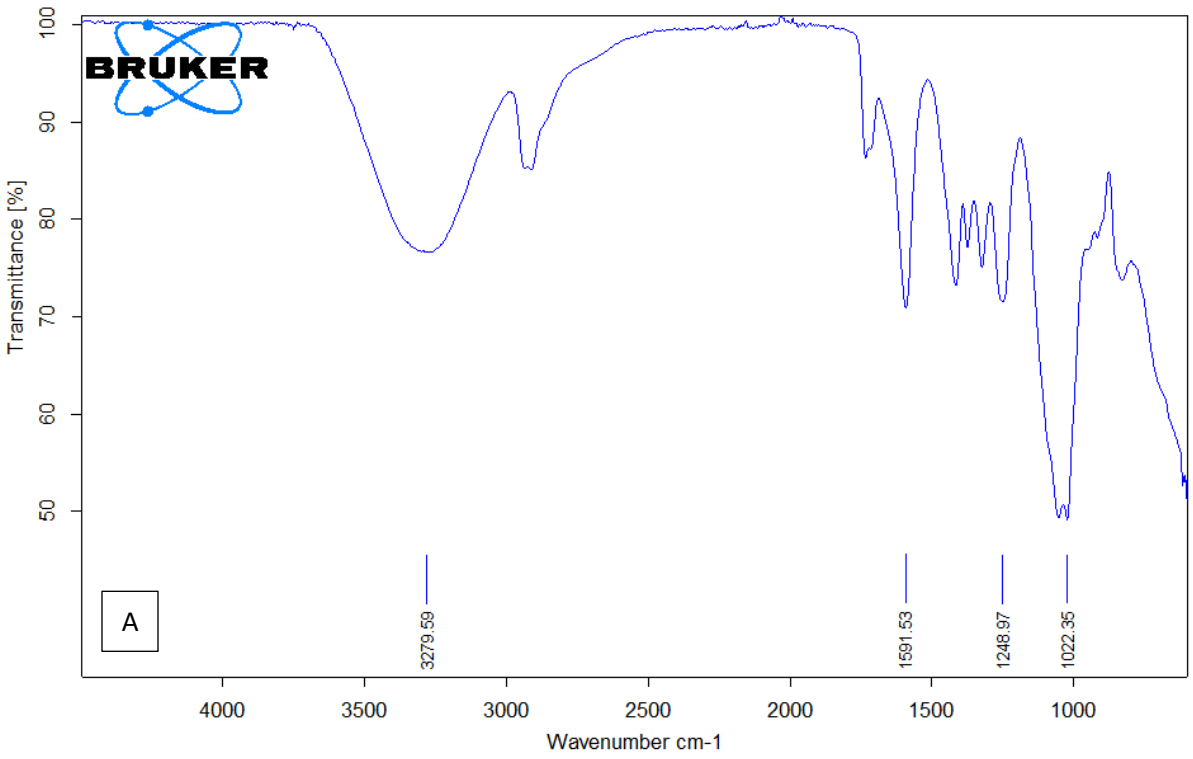

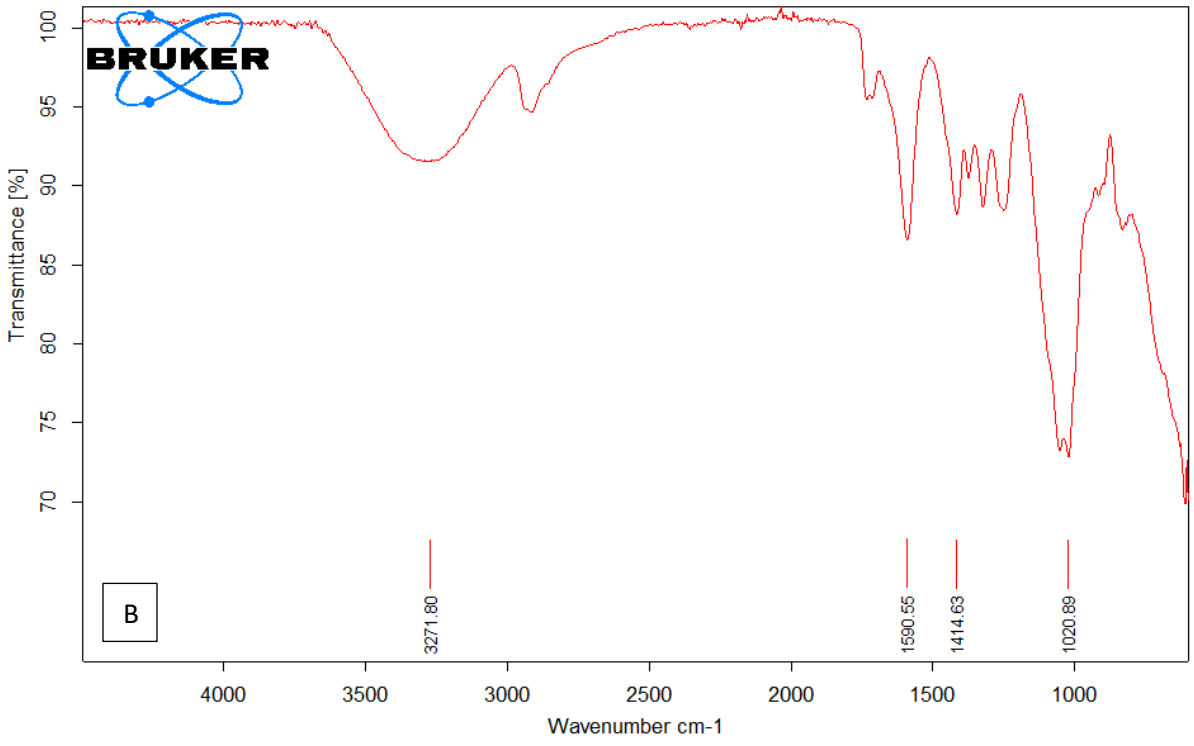
BRUKER
Transmittance [%]
100
95
90
85
80
75
70
B
3271.80
1590.55
1414.63
1020.89
4000
3500
3000
2500
2000
1500
1000
Wavenumber cm-1

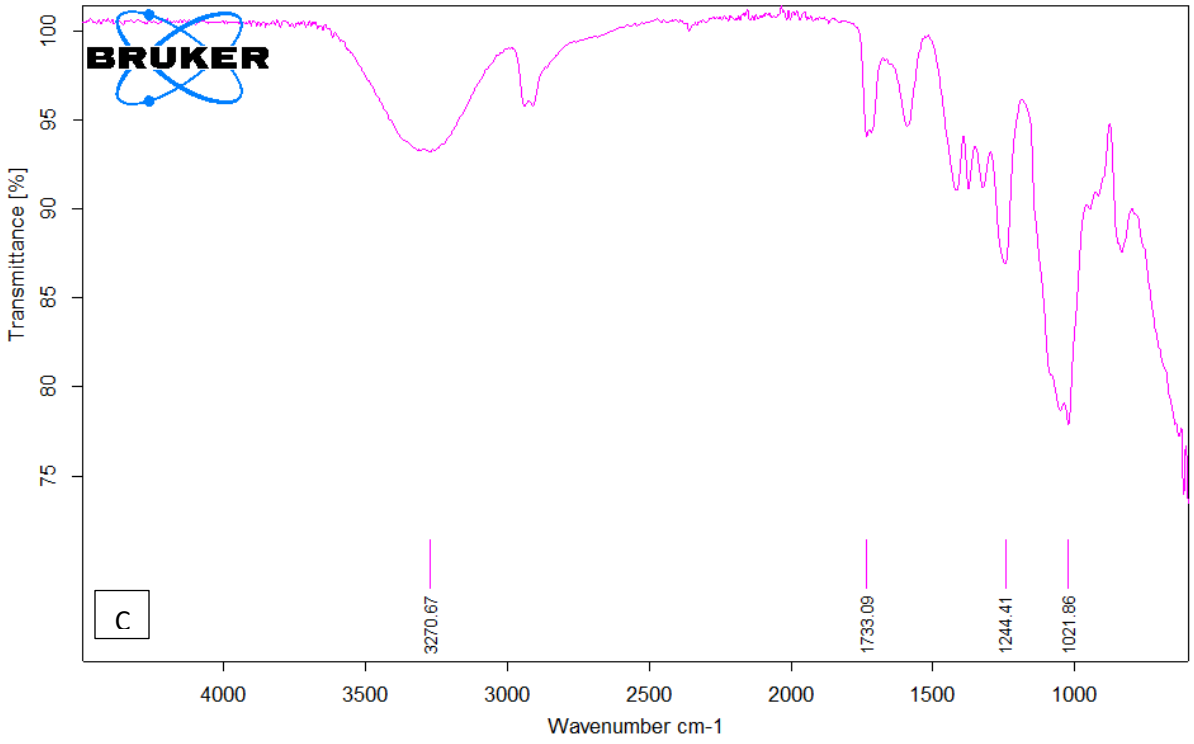
BRUKER
Transmittance [%]
100
95
90
85
80
75
C
3270.67
1733.09
1244.41
1021.86
4000
3500
3000
2500
2000
1500
1000
Wavenumber cm-1

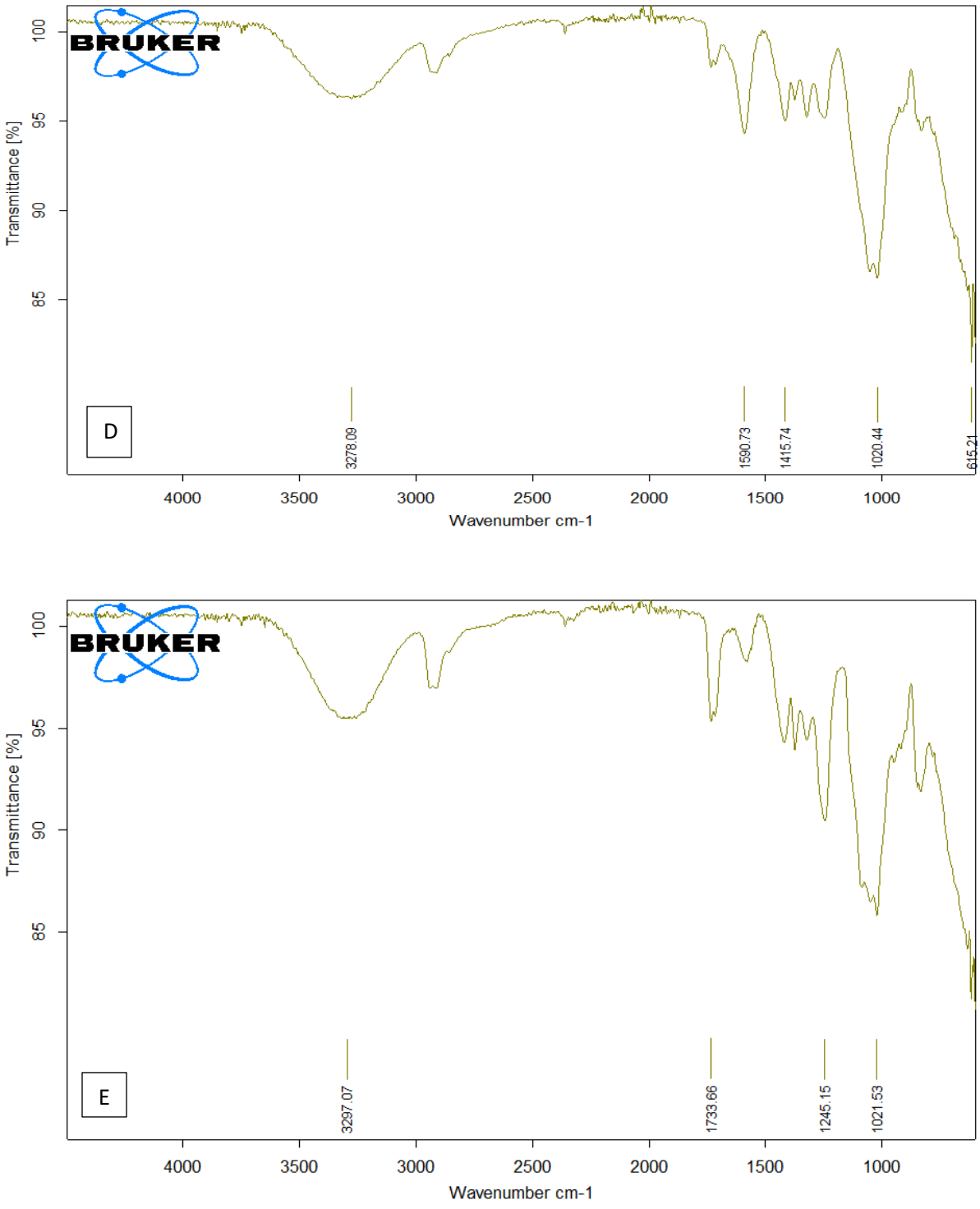

Fig (4.7): FTIR spectra for (CMC-PVA-Mg-Chlorophyll) nanocomposite: (A) (CMC-PVA) blend, (B) 2wt% Mg-Chlorophyll,(C) 4wt% Mg-Chlorophyll, (D) 6wt% Mg-Chlorophyll and 8wt.%Mg-Chlorophyll

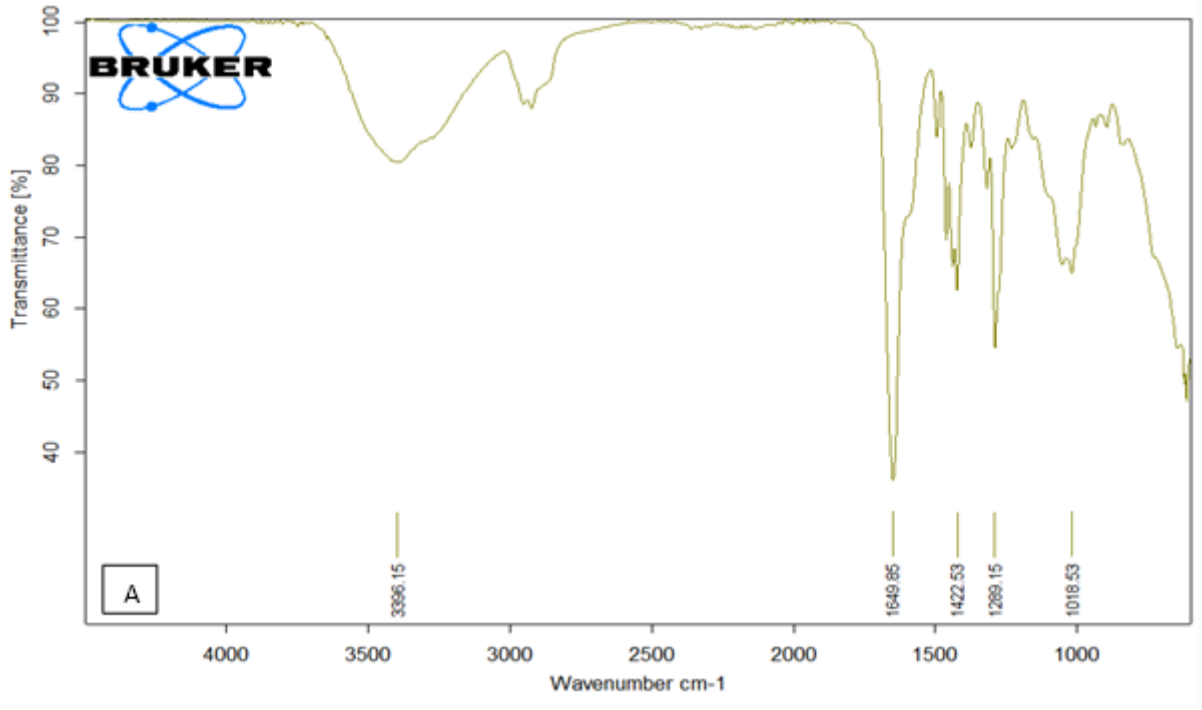
BRUKER
Transmittance [%]
100
90
80
70
60
50
40
A
3396.15
1649.85
1422.53
1289.15
1018.53
4000
3500
3000
2500
2000
1500
1000
Wavenumber cm-1

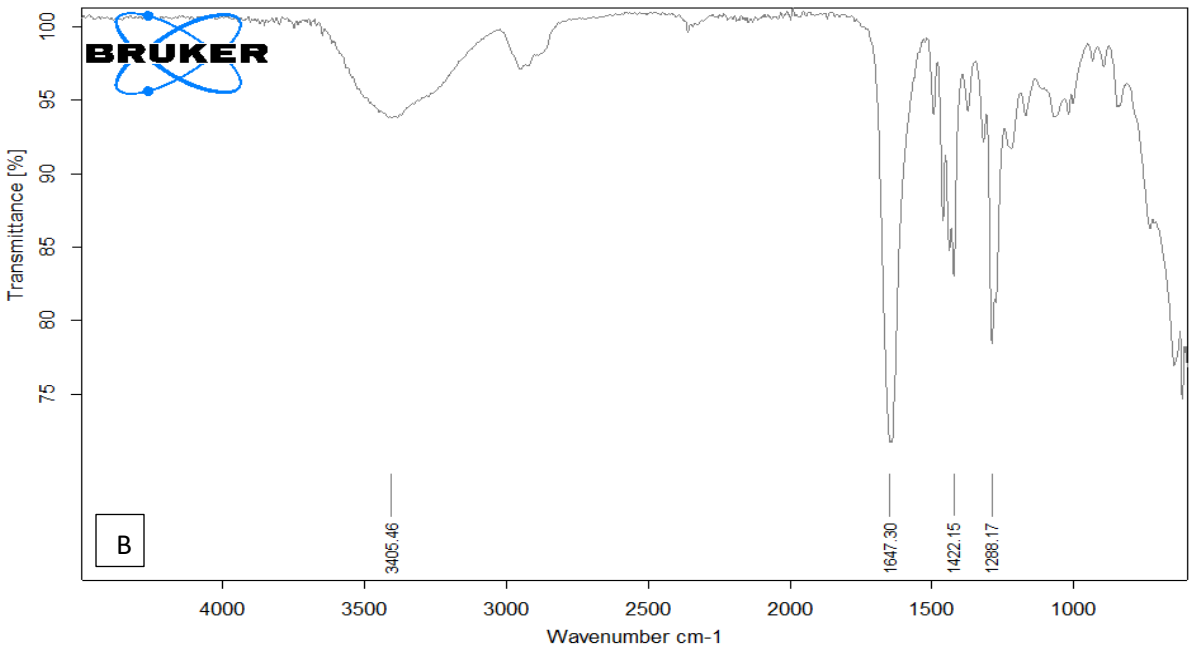
BRUKER
Transmittance [%]
100
95
90
85
80
75
B
3405.46
1647.30
1422.15
1288.17
4000
3500
3000
2500
2000
1500
1000
Wavenumber cm-1

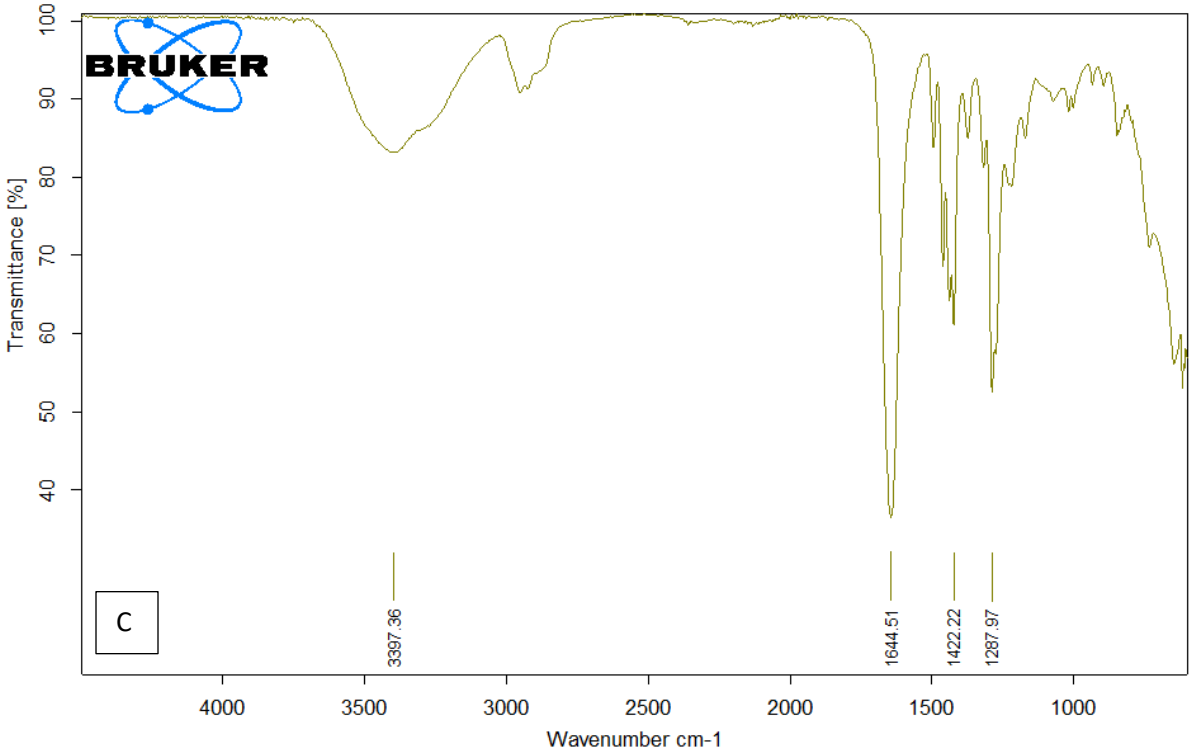
BRUKER
Transmittance [%]
100
90
80
70
60
50
40
C
3397.36
1644.51
1422.22
1287.97
4000
3500
3000
2500
2000
1500
1000
Wavenumber cm-1

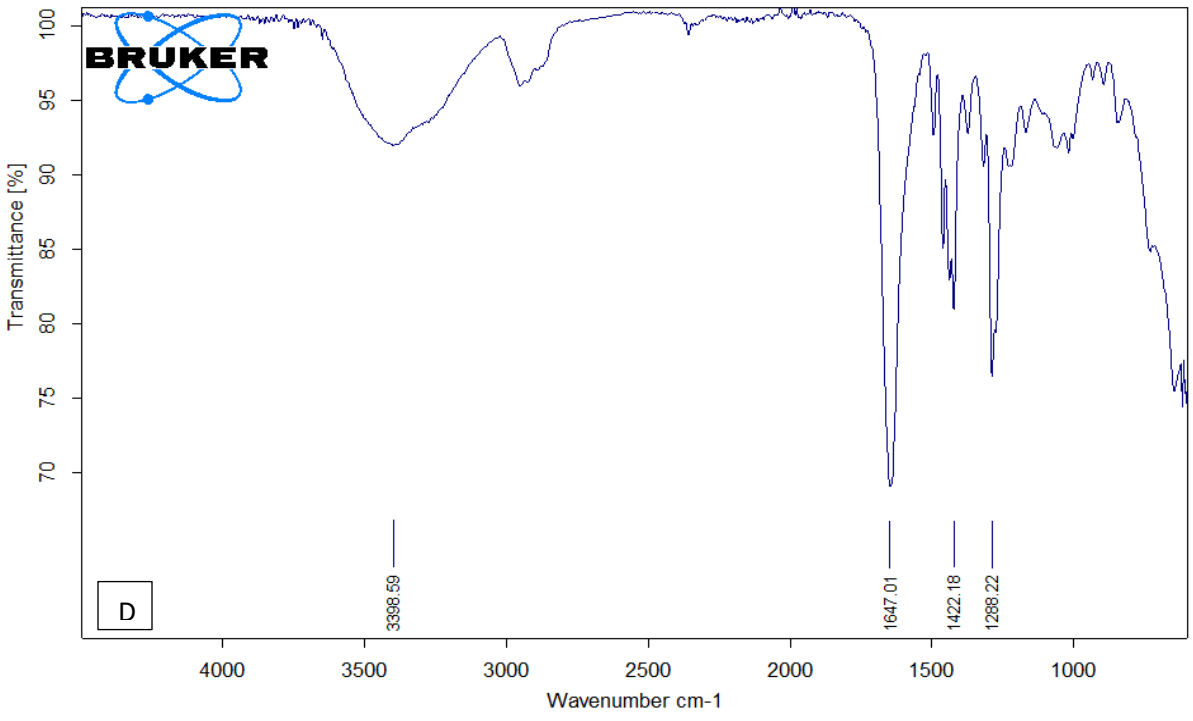
BRUKER
Transmittance [%]
100
95
90
85
80
75
70
D
3398.59
1647.01
1422.18
1288.22
4000
3500
3000
2500
2000
1500
1000
Wavenumber cm-1

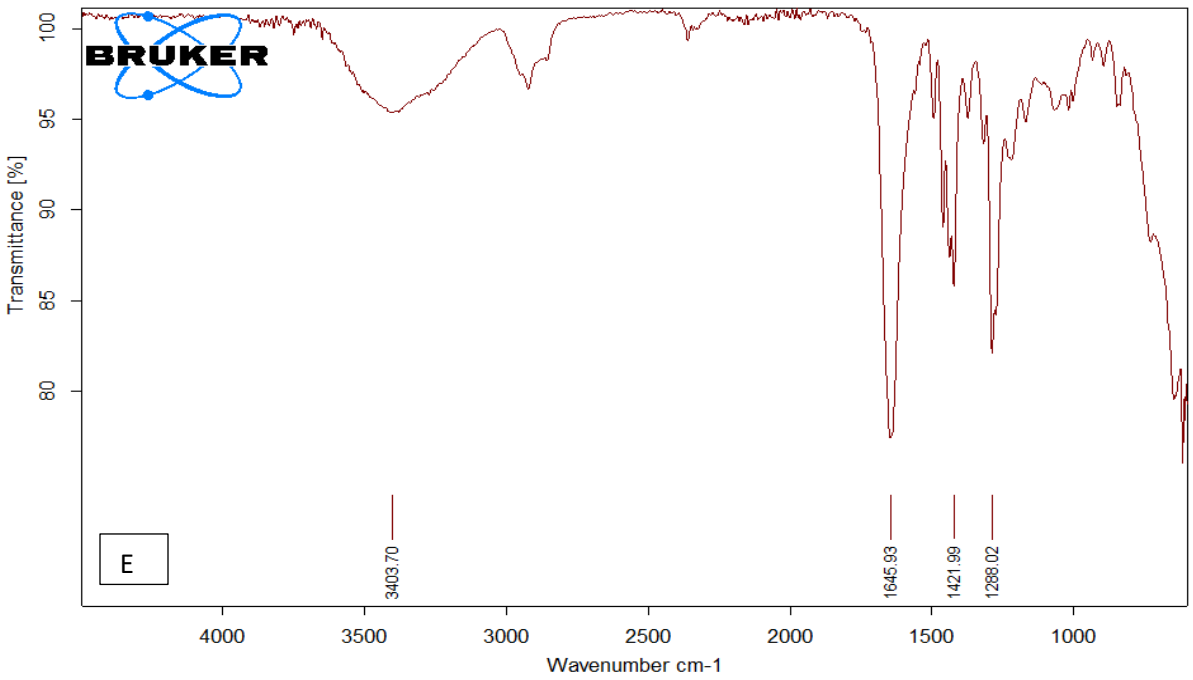

Fig (4.8): FTIR spectra for (CMC-PVP-Mg-Chlorophyll) nanocomposite: (A) (CMC-PVP) blend, (B) 2wt% Mg-Chlorophyll,(C) 4wt% Mg-Chlorophyll, (D) 6wt% Mg-Chlorophyll and 8wt.%Mg-Chlorophyll

4.3 The Optical Properties of (CMC/PVA/Mg-Chlorophyll) and (CMC/PVP/Mg-Chlorophyll) nanocomposite

4.3.1. The absorbance

The absorption of (CMC/PVA/Mg-Chlorophyll) and (CMC/PVP/ Mg-Chlorophyll) nanocomposite with various content of Mg-Chlorophyll Pigments (2, 4, 6 and 8 wt.%) were recorded at wavelengths range (200-1100) nm at room temperature. Figures (4.9) and (4.10) shows the absorption for (CMC/PVA/Mg-Chlorophyll) and (CMC/PVP/Mg-Chlorophyll) nanocomposites with wavelength of the incident light respectively. The absorption peaks in the blue-violet region (400 nm) and the red-infrared region (680 nm) of the electromagnetic spectrum which due to arise from the $\pi \rightarrow \pi^*$ transitions, where π^* denotes the excited state.

In addition to these $\pi \rightarrow \pi^*$ transitions, electrons can also be excited to the HOMO from orbitals lower than LUMO [109,110].

From this figure, it can be noted that the absorbance rises with rising content of Mg-Chlorophyll. This is due to donor level electrons being excited to the conduction band at high energies. Also, because photons provide enough energy to react with atoms, an electron can be excited from a lower to a higher energy level by absorption an established photon [111]. The researchers are affected by this behavior [112,113] The results agree with the results of the previous researchers [55].

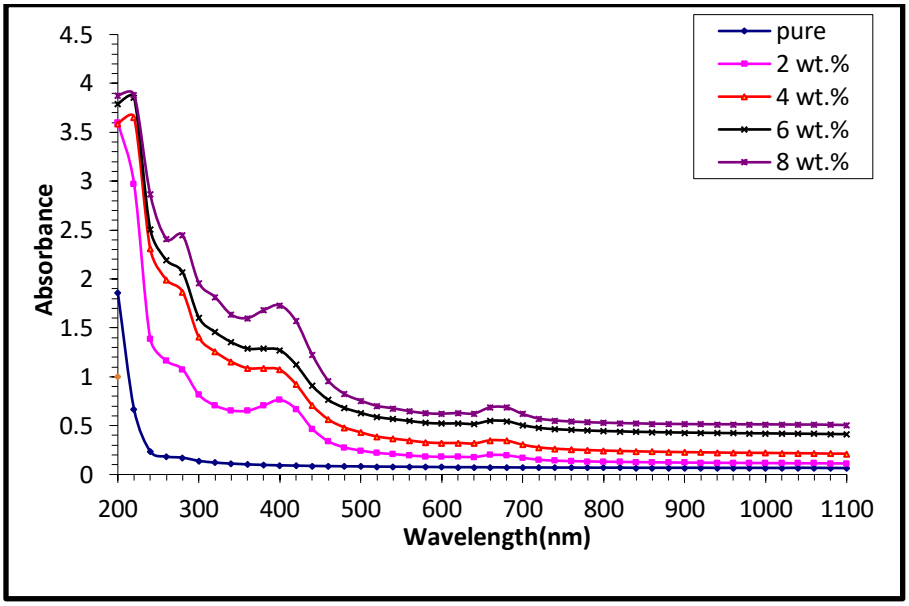

Fig.(4.9): The absorbance as a function of wavelength of (CMC/PVA/Mg-Chlorophyll) nanocomposite with different content.

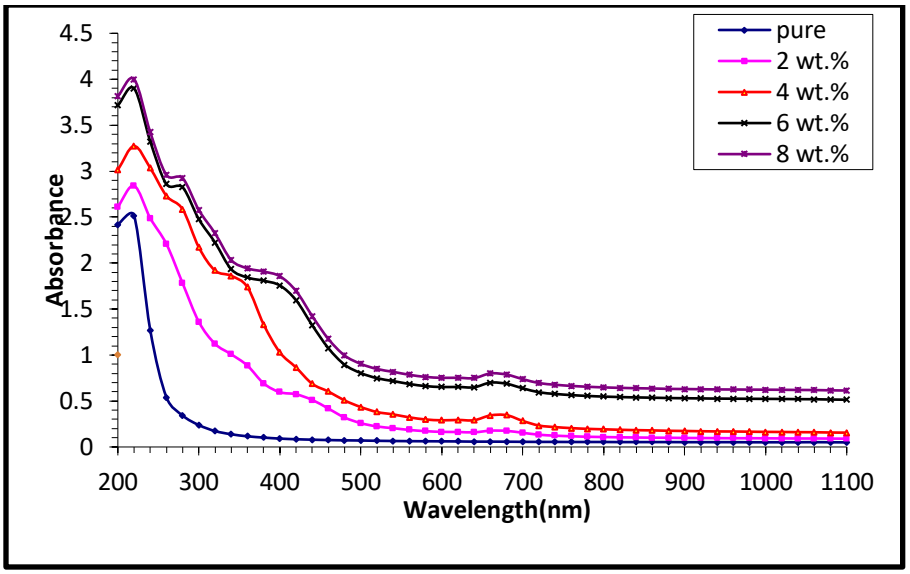

Fig.(4.10): The absorbance as a function of wavelength of (CMC/PVP/ Mg-Chlorophyll) nanocomposite with different content.

4.4.2 The transmittance

The transmittance of (CMC/PVA/Mg-Chlorophyll) and (CMC/PVP/ Mg-Chlorophyll) nanocomposite with wavelength are shown in figs.(4.11),(4.12). The transmittance decreased with increasing concentration of Mg-Chlorophyll which is due to the agglomeration of nanoparticles with rising content of Mg-Chlorophyll [114].

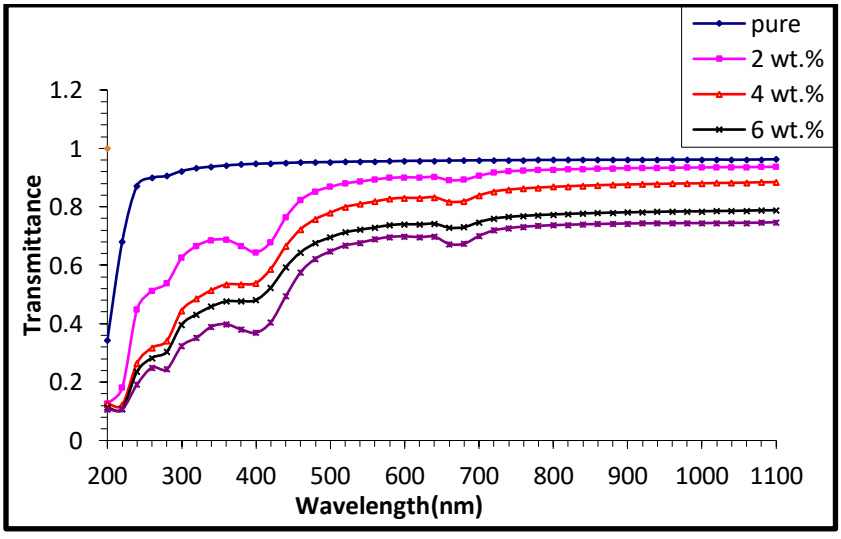

Fig.(4.11): Variation transmittance of (CMC/PVA/Mg-Chlorophyll) nanocomposite with the wavelengths.

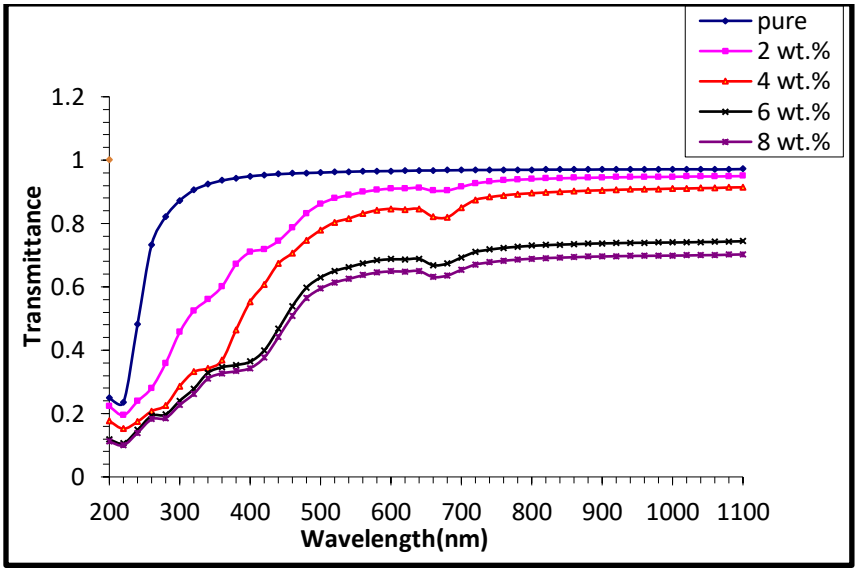

Fig.(4.12): Variation transmittance of (CMC/PVP/ Mg-Chlorophyll) nanocomposite with the wavelengths.

4.3.3 The absorption coefficient (α)

The absorption coefficient (α) of nanocomposites were calculated by equation (2-6). The absorption coefficient of (CMC/PVA/Mg-Chlorophyll) and (CMC/PVP/ Mg-Chlorophyll) nanocomposite versus photon energy of the incident light are shown in Figures (4.13) and (4.14) respectively. The absorption coefficient might help you figure out what kind of electron transition you're dealing with [115,116].

It is assumed that direct electron transitions occur when the material's absorption coefficient is large ($>10^4$) cm^{-1}. When the material's absorption coefficient is low (10^4 cm^{-1}), an indirect transition of electrons is assumed. The values of α of (CMC/PVA/Mg-Chlorophyll) and (CMC/PVP/ Mg-Chlorophyll) nanocomposite, the transition of electron is indirect. The α of nanocomposites increased with the increasing concentration of Mg-Chlorophyll, this is due to the rise of number of charge carriers and therefore rising the absorbance and

absorption coefficient for (CMC/PVA/Mg-Chlorophyll) and (CMC/PVP/ Mg-Chlorophyll) nanocomposites [117].

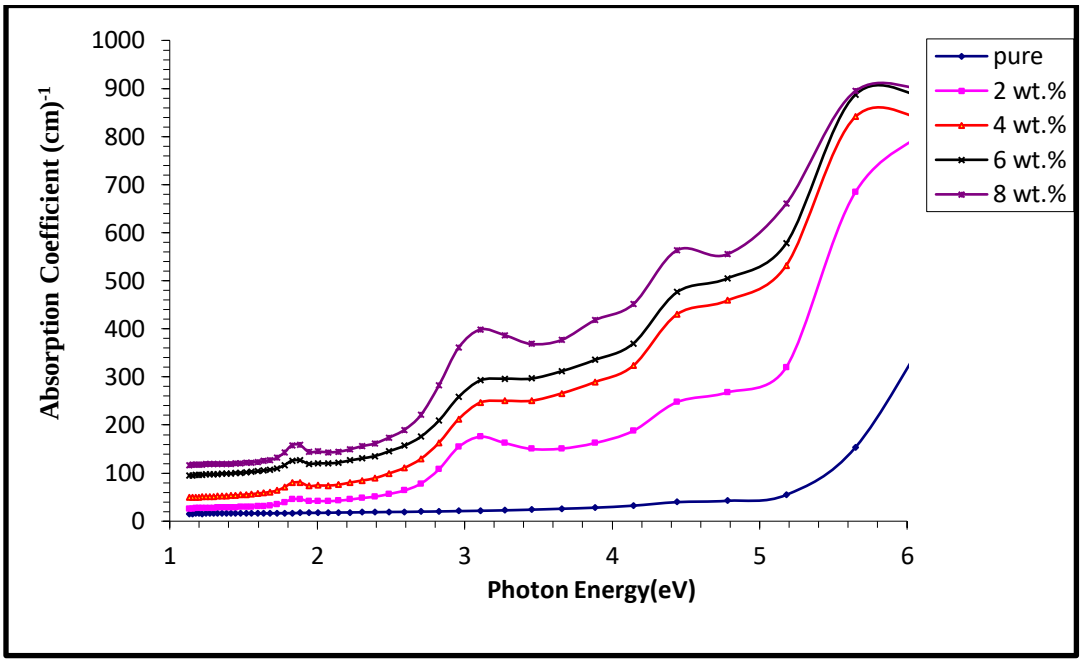

Fig.(4.13) : The variation absorption coefficient of (CMC/PVA/Mg-Chlorophyll) nanocomposite with the photon energies.

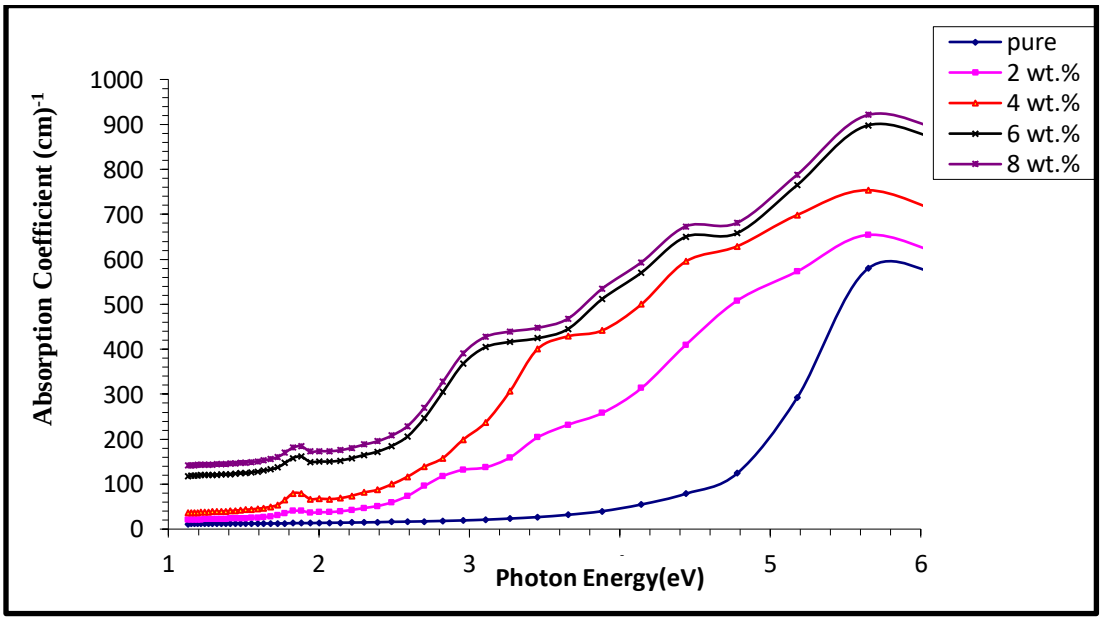

Fig.(4.14) : The variation absorption coefficient of (CMC/PVP/ Mg-Chlorophyll) nanocomposite with the photon energies.

4.3.4 The allowed indirect energy gap

The energy band gap of nanocomposites was calculated by equation (2-9). The energy gap for allowed indirect transitions of (CMC/PVA/Mg-Chlorophyll) and (CMC/PVP/ Mg-Chlorophyll) nanocomposites are explain in Figures (4.15) and (4.16) respectively.

We may find the energy gap for the indirect transition by plotting the data or tang cut from the top of the curve to the (x axis) at (hv) [118]. From this figure, the E_g for allowed and forbidden indirect transitions are reduce with the rises concentration of the Mg-Chlorophyll. This action is due to the formation of levels in the E_g and therefore, these local levels reduce the energy gap with rise of the Mg-Chlorophyll content [119]. The value of the E_g of nanocomposites are listed in Table (1). The results agree with the results of the previous researchers [55].

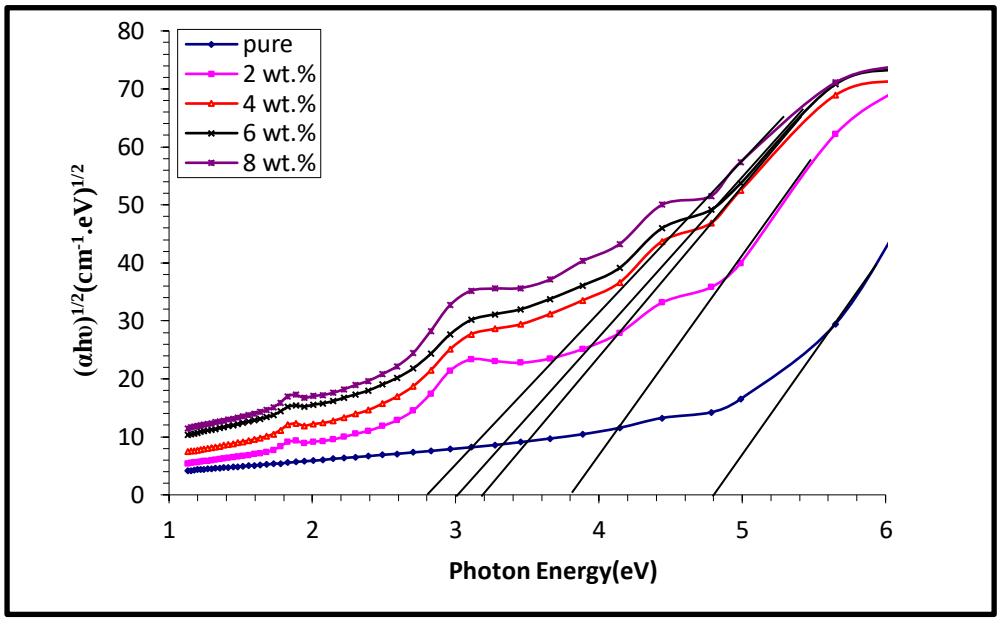

Fig.(4.15): The E_g for the allowed indirect transition $(\alpha h\nu)^{1/2}$ $(cm^{-1}.eV)^{1/2}$ of (CMC/PVA/Mg-Chlorophyll) nanocomposite

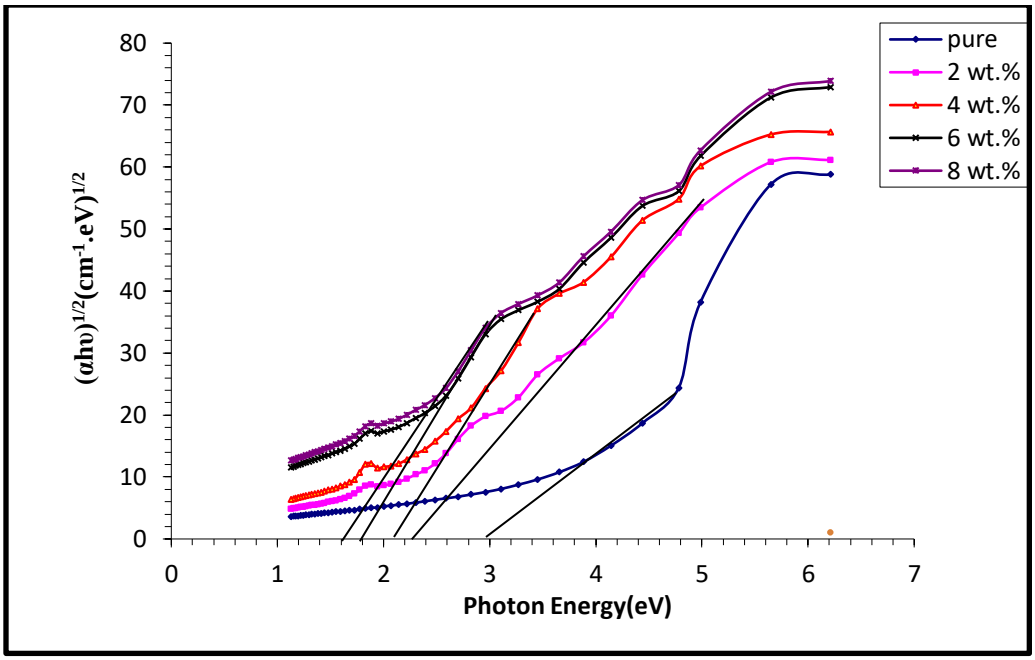

Fig.(4.16): The E_g for the allowed indirect transition $(\alpha h\nu)^{1/2}$ $(cm^{-1}.eV)^{1/2}$ of (CMC/PVP/ Mg-Chlorophyll) nanocomposite

Table (4.1): The values allowed E_g of (CMC/PVA/Mg-Chlorophyll) and (CMC/PVP/ Mg-Chlorophyll) nanocomposite

Con. of Mg-Chlorophyll wt%	Eg allowed indirect for the (CMC/PVA/Mg-Chlorophyll)(eV)	Eg allowed indirect for the (CMC/PVP/ Mg-Chlorophyll)(eV)
0	4.8	3
2	3.8	2.3
4	3.2	2.1
6	3	1.8
8	2.8	1.6

4.3.5 The extinction coefficient (K_o)

The extinction coefficient (K_o) was calculated by using the equation (2-14). Figures (4.17) and (4.18) explain the extinction coefficient of (CMC/PVA/Mg-Chlorophyll) and (CMC/PVP/ Mg-Chlorophyll) nanocomposites versus of wavelength respectively. It is observed that the K of nanocomposites increased with the increasing of the Mg-Chlorophyll content, which is due to the increase in optical absorption and photons distribution in the (CMC/PVP) and (CMC/PVP) polymer matrix respectively [120].

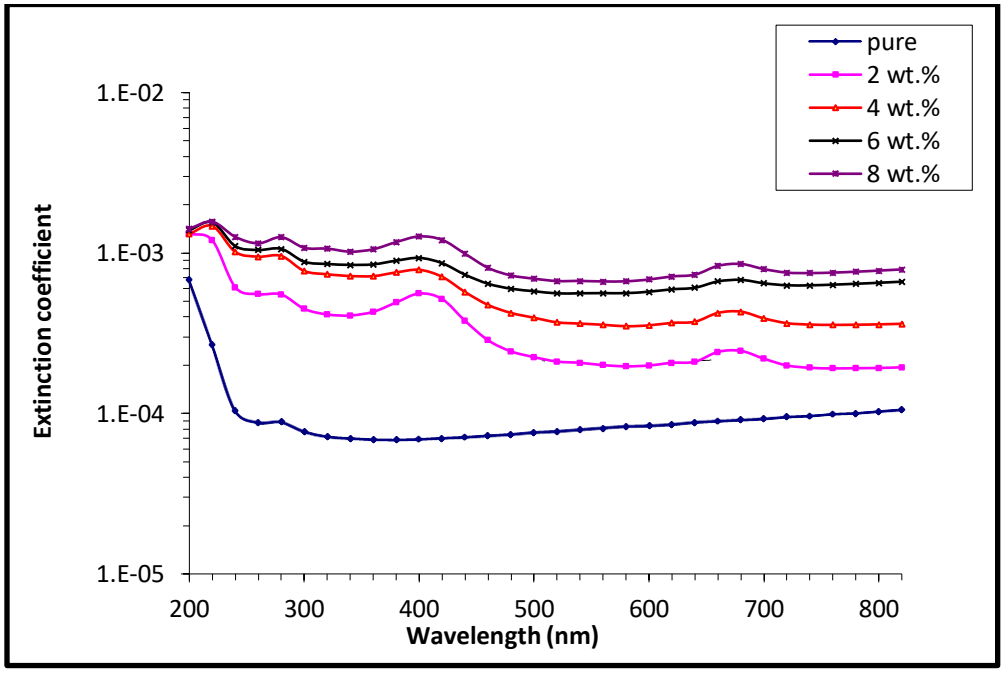

Fig. (4.17): Variation of K for (CMC/PVA/Mg-Chlorophyll) nanocomposite with the wavelength

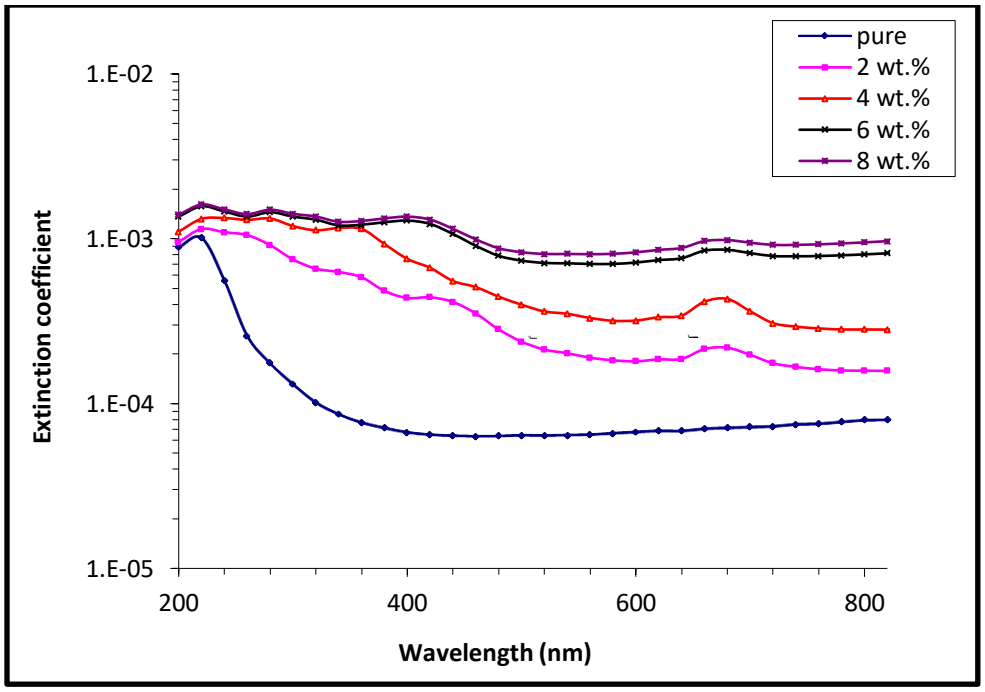

Fig.(4.18): Variation of K for (CMC/PVP/ Mg-Chlorophyll) nanocomposite with the wavelength

4.3.6 The refractive index (n)

The refractive index is calculated by using equation (2-12). The refractive index of(CMC/PVA/Mg-Chlorophyll) and (CMC/PVP/Mg-Chlorophyll) nanocomposites versus with wavelength are shown in Figures (4.19) and (4.20) respectively. It is obtained that the refractive index of increase with the increasing of the content of Mg-Chlorophyll. This action due to the rise of the density of nanocomposites [121,122].

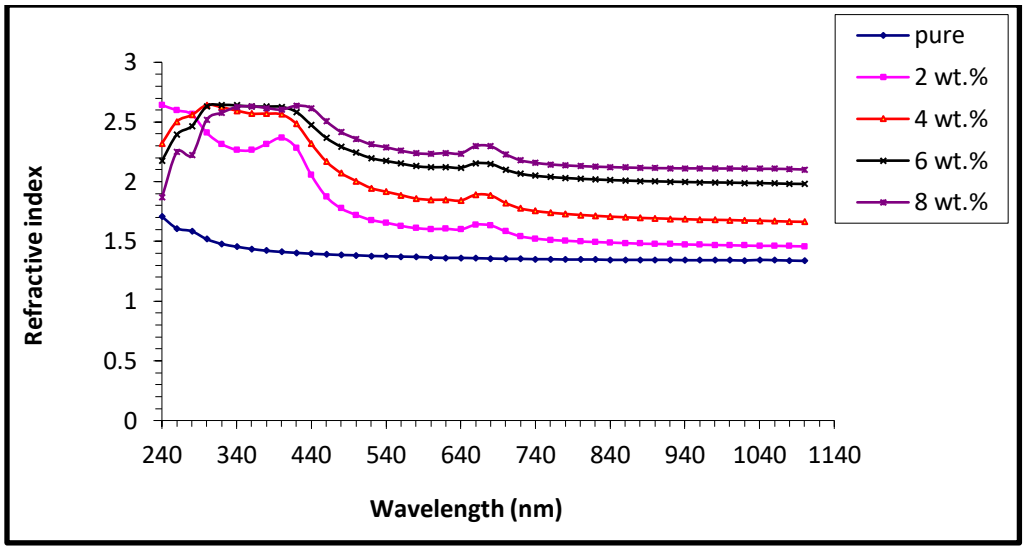

Fig.(4.19) : Variation of n for of (CMC/PVA/Mg-Chlorophyll) nanocomposites with wavelength

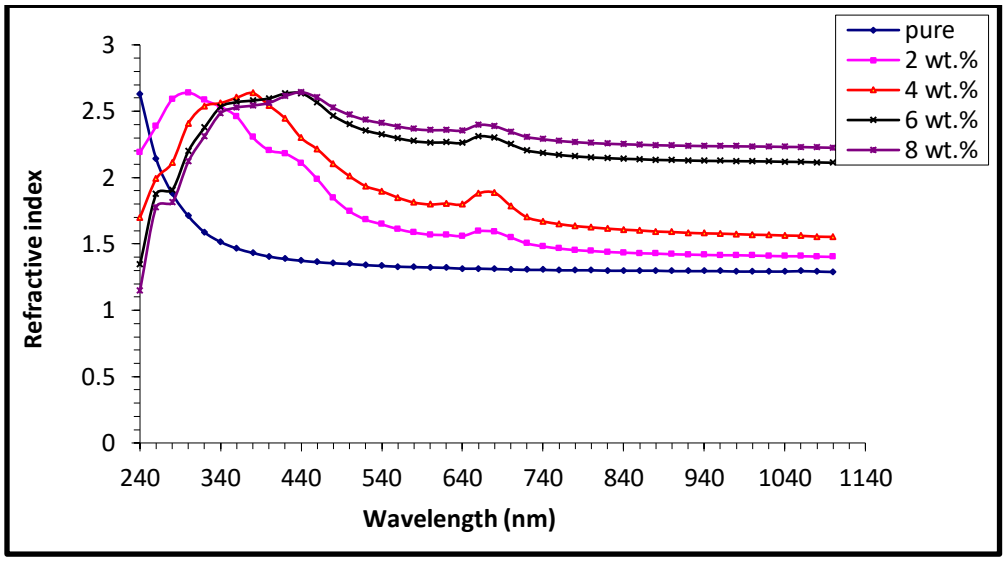

Fig.(4.20) : Variation of n for of (CMC/PVP/Mg-Chlorophyll) nanocomposites with wavelength

4.3.7 The real (ε_1) and imaginary (ε_2) parts of dielectric constant

By using the equations (2-18) and (2-19), the real (ε_1) and imaginary (ε_2) parts of dielectric constant were calculated. The ε_1 with the wavelength for (CMC/PVA/Mg-Chlorophyll) and (CMC/PVP/Mg-Chlorophyll) nanocomposites are explain in Figures (4.21) and (4.22) and ε_2 with the wavelength for the (CMC/PVA/Mg-Chlorophyll) and (CMC/PVP/Mg-Chlorophyll) nanocomposites

are explain in Figures (4.23) and (4.24) respectively. From this figure, the ε_1, ε_2 of the nanocomposite are increase with the increasing of Mg-Chlorophyll content. The increase in electrical polarization related to the contribution of nanoparticles content in the sample caused this finding [123]. Also due to the ε_1 depends on refractive index because the effect of extinction coefficient is small, whereas the ε_2 depends on extinction coefficient [124].

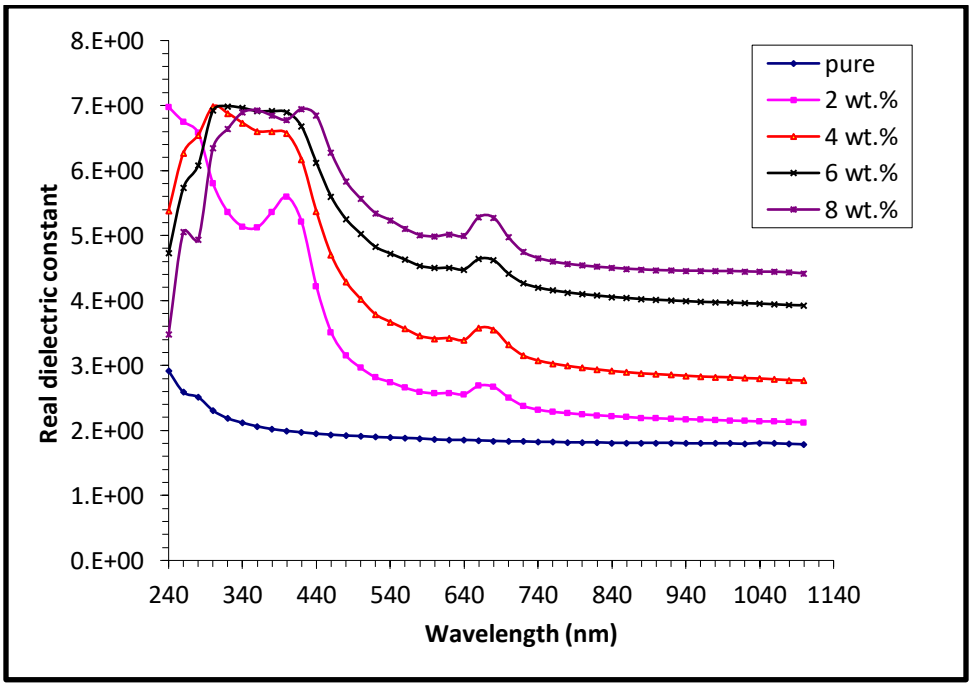

Fig.(4.21): Variation of ε_1 of (CMC/PVA/Mg-Chlorophyll) nanocomposites with the wavelength

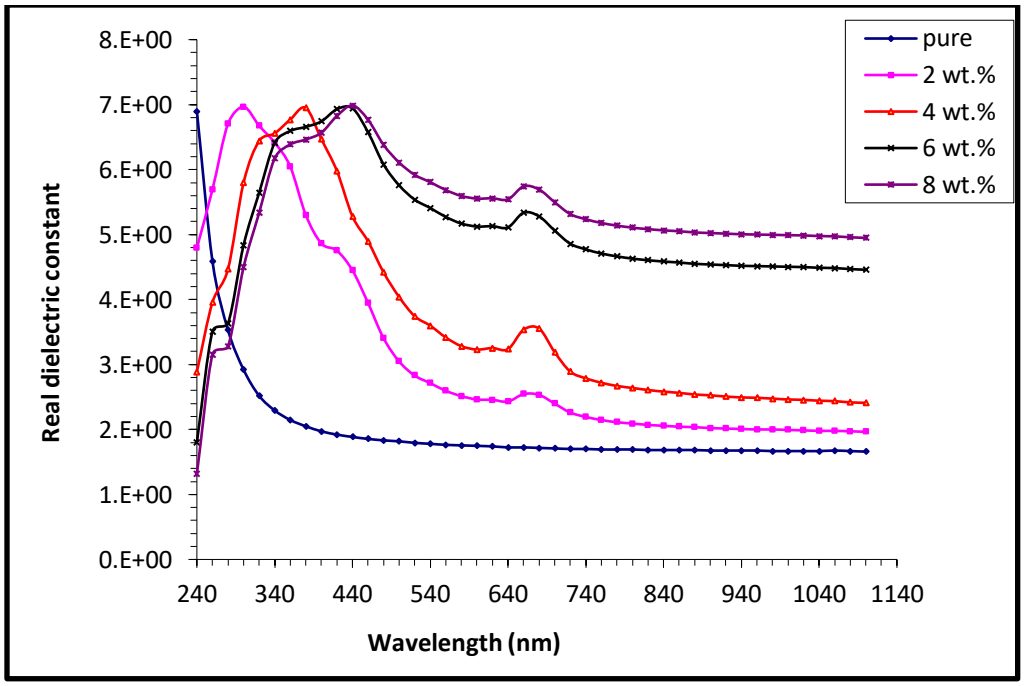

Fig. (4.22): Variation of ε_1 of (CMC/PVP/Mg-Chlorophyll) nanocomposites with the wavelength

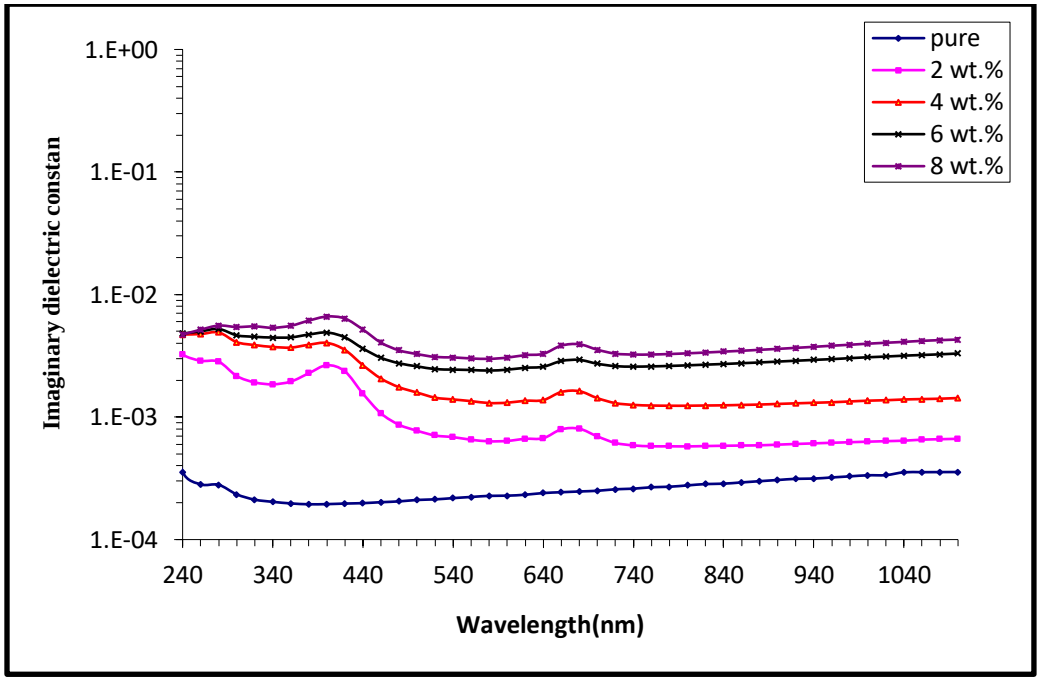

Fig.(4.23): Variation ε_2 of (CMC/PVA/Mg-Chlorophyll) nanocomposites with the wavelength.

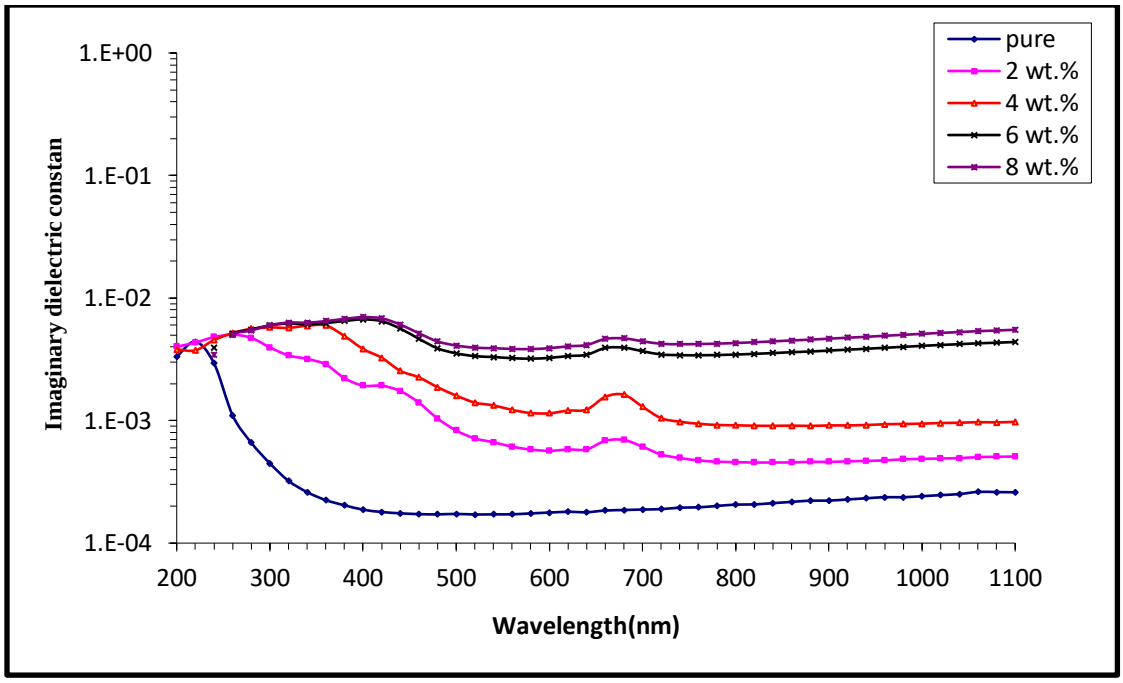

Fig.(4.24): Variation ε_2 of (CMC/PVP/Mg-Chlorophyll) nanocomposites with the wavelength.

4.3.8 The optical conductivity (σ_{op})

The optical conductivity (σ_{op}) was calculated from the equation (2- 20). The optical conductivity of (CMC/PVA/Mg-Chlorophyll) and (CMC/PVP/Mg-Chlorophyll) nanocomposites with a wavelength are explain in Figures (4.25) and (4.26) respectively. From this figure, the σ_{op} increase with increasing concentration of Mg-Chlorophyll which is related to the formation of localized levels in the energy gap, rising Mg-Chlorophyll content induced a rise in the density of localized phases in the band structure therefore, an increase in the absorption coefficient suggests an increase in σ_{op} of the nanocomposites. This outcome is consistent with previous study [125].

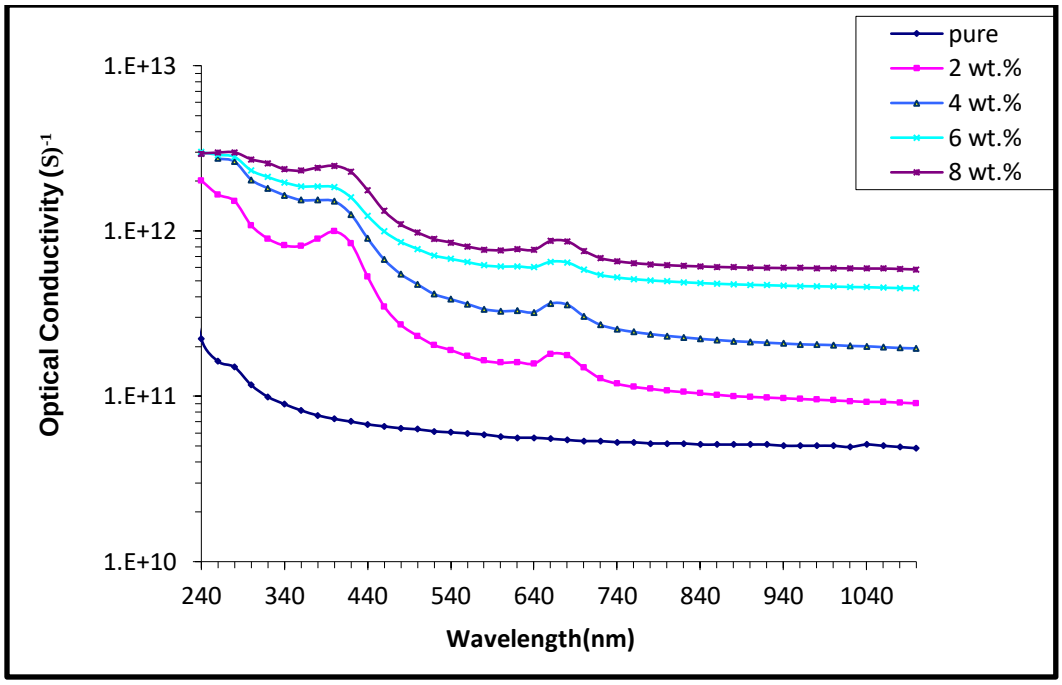

Fig.(4.25): Variation σ_{op} of (CMC/PVA/Mg-Chlorophyll) nanocomposites with the wavelength.

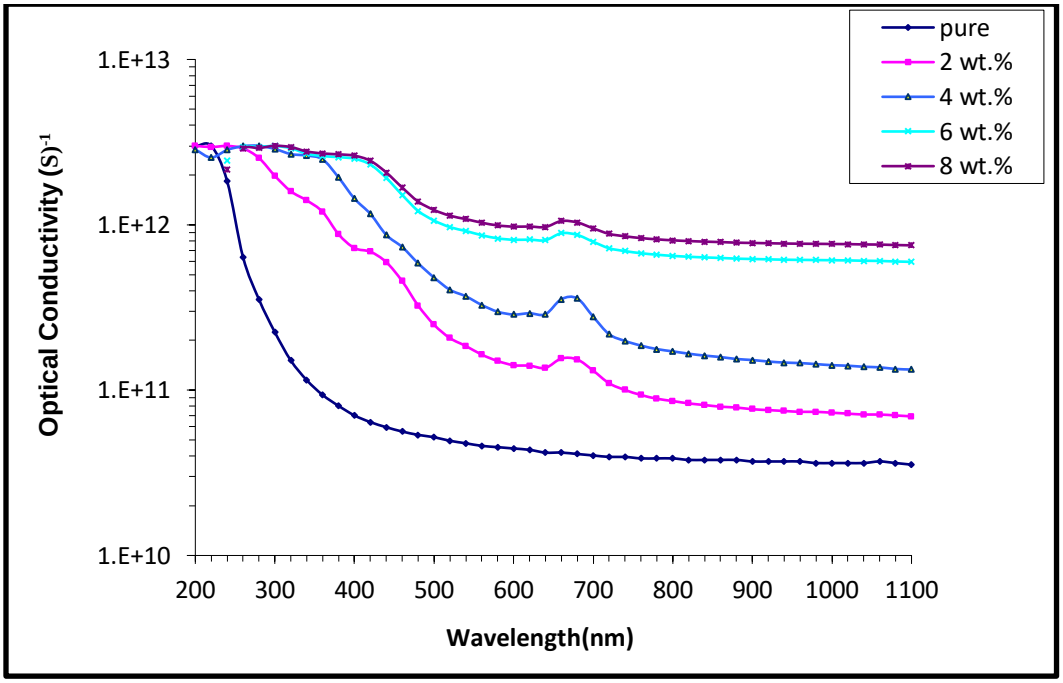

Fig.(4.26): Variation σ_{op} of (CMC/PVP/Mg-Chlorophyll) nanocomposites with the wavelength.

4.4 Conclusion

The following points are concluded:

1- The XRD obtained that the semicrystalline structure of CMC/PVA and CMC/PVP polymer blend and with added different concentration of Mg-Chlorophyll Pigments (2, 4, 6 and 8 wt.%), the intensity increased and there are no peaks appears, which due to the low concentration added to the CMC/PVA and CMC/PVP polymer blend and also due to the broad peaks of the CMC/PVA and CMC/PVP which disappear all peaks.

2- From the FESEM and the optical microscope images showed the Mg-Chlorophyll) form a continuous network inside the CMC/PVA and CMC/PVP polymer blend at concentration of 8 wt.%.

3- FTIR spectra shows shift in some bonds and change in the intensities and proved that there are no interactions between the CMC/PVA and CMC/PVP polymer matrix and Mg-Chlorophyll nanoparticles.

4- The optical properties exhibited that the absorbance, absorption coefficient, extinction coefficient, refractive index, real and imaginary parts of dielectric constants and optical conductivity are increased with increasing the concentration of Mg-Chlorophyll nanoparticles, while the transmittance and the indirect energy gap decreased with the increasing concentration of Mg-Chlorophyll nanoparticles. From this result, the CMC/PVP/Mg-Chlorophyll) nanocomposites exhibit the best improving structural, morphological and optical properties that can be used for solar cell and photodetector application.

4.5 Future Works

The following suggests for future work:

1. Study effect of Mg-Chlorophyll nanoparticles on the structural, optical and electrical properties for (PMMA/PS) polymer blend

2. Effect of the prepared Mg-Chlorophyll nanoparticle on structural and morphological properties of polyacrylamide (PAAm).

4. Apply these nanocomposites as the photodetector.

References

References

1. D. Feldman, " Polymer history", Designed monomers and polymers, 11(1), 1-15, (2008).

2. C. Tanford, and J. Reynolds, " Nature's robots: a history of proteins", OUP Oxford, (2003).

3. B. Adhikari, , D. De, , and S. Maiti, " Reclamation and recycling of waste rubber", Progress in polymer science, 25(7), 909-948, (2000).

4. H. Ringsdorf, "Hermann Staudinger and the future of polymer research jubilees—beloved occasions for cultural piety", Angewandte Chemie International Edition, 43(9), 1064-1076, (2004).

5. S. R. Forrest, " The path to ubiquitous and low-cost organic electronic appliances on plastic", nature, 428(6986), 911-918, (2004).

6. S. Mustafa, “Engineering Chemistry”, Library of Arab society for pub. and dis, Jordan, (2008).

7. Teraoka, "Polymer Solutions: An Introduction to Physical Properties", John Wiley and Sons, Inc,(2002).

8. K. W. Allen, D.I Bower, "An introduction to polymer physics", Materials Science and Technology, 19(5), 676. (2003).

9. A. Muheisin, "Study of Electrical Conductivity for Amorphous and Semi crystalline Polymers Filled with Lithium Fluoride Additive", M.Sc. Thesis, University of Mustansiriah, College of Science, (2009).

10. J. Schultz, “Polymer materials science,” Prentice-Hall Englewood Cliffs, NJ, (1974).

11. L. H. Howared, "Introduction to Physical Polymer Science", 4thEd., printed in United States of America, (2006).

12. I. David Bower, "An Introduction to Polymer Physics", Cambridge University Press, ISBN: 9780521631372, P. 464,(2002).

13. J. W. Nicholson, "The Chemistry of Polymers", the Royal Society of Chemistry, ISBN 978-0-85404-684-3, P. 178, (2006).

14. J. J. Scobboand L. A. Goettler, “Applications of polymer alloys and blends”, Kluwer Academic Publishers , (2003).

15. J. E. Mark, “Physical properties of polymers handbook”, Springe, Vol. 107, p.825, (2007).

16. F. W. Billmeyer, " Textbook of polymer science", John Wiley and Sons, (1984).

17. J. M. G. Cowie, “Polymers: Chemistry and Physics of Modern Materials”, Glasgow, (2007).

18. S. Amin, and M. Amin, “Thermoplastic Elastomeric (Tpe) Materialsand Their Use in Outdoor Electrical Insulation”, Rev. Adv. Mater. Sci.,Vol. 29, pp.15-30, (2011).

19. A. Long ," Composites Forming Technologies" , Cambridge University, England , (2007).

20. S. S. Pendhari, T. Kant and Y. M. Desai, " Application of polymer composites in civil construction": A general review. Composite structures, 84(2), 114-124,(2008).

21. K. Malhotra, and S. Rani, "A Review on Mechanical Characterization of Natural Fiber Reinforced Polymer Composites. Journal of Engineering Research and Studies, 3, 75-80.(2012).

22. R. R. Nagavally, "Composite materials-history, types, fabrication techniques ,advantages, and applications." Int J Mech Prod Eng 5.9: 82-7(2017).

23. S. K. Saxena, "Polyvinyl alcohol (PVA)", Chemical and Technical Assessment, 1(3), 3-5, (2004).

24. P. C. Hiemenz, and T. P. Lodge, "Polymer chemistry", CRC press (2007).

25. S. G. Rathod, R. F. Bhajantri, V. Ravindrachary, , T. Sheela, , P. K. Pujari, J. Naik, and B. Poojary, " Pressure sensitive dielectric properties of TiO_2 doped PVA/CN-Li nanocomposite". Journal of Polymer Research, 22(2), 1-14 , (2015).

26. E. Sheha, , H. Khoder, T. S. Shanap, , M. G. El-Shaarawy, , and El M. K. Mansy, "Structure, dielectric and optical properties of p-type (PVA/CuI) nanocomposite polymer electrolyte for photovoltaic cells", Optik, 123(13), 1161-1166, (2012).

27. C. M. Hassan, , and N. A. Peppas," PVA Hydrogels, Anionic Polymerisation Nanocomposites", Biopolymers, 37-65, (2000).

28. S. Mallakpour, and A. Barati, "Efficient preparation of hybrid nanocomposite coatings based on poly (vinyl alcohol) and silane coupling agent modified TiO_2 nanoparticles", Progress in Organic Coatings, 71(4), 391-398,(2011).

29. C. A. Finch, "Polyvinyl alcohol; properties and applications",John Wiley and Sons, (1973).

30. A. Gautam, and S. Ram, "Preparation and thermomechanical properties of Ag-PVA nanocomposite films", Materials Chemistry and Physics, 119(1-2), 266-271,(2010).

31. A. J. Mohammed, and S. H. Al-nesrawy, "Nano Ferrite Incorporated Poly (Vinyl Pyrrolidone (PVP)/Poly (Vinyl Alcohol (PVA) Blend: Preparation and Investigation of Structural, Morphological and Optical Properties", NeuroQuantology, 20(3), 251-258.), (2022).

32. S. S. Chiad, S. F. Oboudi, K. H. Abass and N. F. Habubi, "Characterization of Silver/Polyvinyl Alcohol (Ag/PVA) Films prepared by Casting Technique", Iraqi J. of Polymers, Vol. 16, No.10-18, (2012).

33. J. H. Koo," Polymer nanocomposites .processing, characterization and applications", McGraw-Hill Nanoscience and Technology Series, New York,(2006).

34. G. K. Veeran and V. B. Guru,"Water Soluble Polymers for Pharmaceutical Applications",Journal of Polymers Vol.3,pp.1972-2009 (2011).

35. A. k. Abbas, R. M. Naife, F. L. Rashid and A. Hashim, "Optical Propertiesof (PVA-PAA-Ag) Nanocomposites", International Journal of Science and Research (IJSR), Vol.4, (2015).

36. R. Tomar and R. C. Sharma, "Studies on Conducting PVP Polymer Composites for A.C Conduction", International Journal of Science, Engineering and Technology Research (IJSETR)3, 3023-3026, (2014).

37. T. H. C. Sallesa and C. B.Lombelloband M. Akira, Electrospinning of Gelatin/Poly (vinyl Pyrrolidone) Blendsfrom Water/Acetic Acid Solutions, Materials Research18, 509-518, (2015).

38. F. Aguilar, B. Dusemund, Galtier, J. Gilbert, D.M. Gott, S. Grilli, R. Gürtler, J. König, C. Lambre, J. C.Larsen, J. C. Leblanc, A. Mortensen, D. Massin, I. Pratt, I.M.C.M. Rietjens, I. Stankovic, Tobback and T. Verguievaand R.A. Woutersen, "Scientific Opinion on The Safety of Polyvinyl Pyrrolidone-vinyl Acetate Copolymer for The Proposed Uses As A Food Additive", EFSA Journal8,(2010).

39. K. Hemalatha, H. Somashe kara and R. Somashekar, Micro-Structure, A.C Conductivity and Spectroscopic Studies of Cupric Sulphate Doped PVA/PVP Polymer Composites, Advances in Materials Physics and Chemistry5, 408-418, (2015).

40. M. Ravi, Y. Pavani, K. K. Kumar, S. Bhavani, A.K. Sharma and V.V.R. N.Rao, "Studies on Electrical and Dielectric Properties of PVP:$KBrO_4$ComplexedPolymer Electrolyte Films", Materials Chemistry and Physics130, 442-448, (2011).

41. E. M. Abdelrazeka, H.M. and Ragabband M. Abdelaziza, "Physical Characterization of Poly (vinylpyrrolidone) and Gelatin Blend Films Doped with Magnesium Chloride", Plastic and Polymer Technology (PAPT)2, (2013).

42. H. Hakim, Z. Al-Ramadhan and A. Hashim, "The Effect of Aluminum Oxide Nanoparticles on the Optical Properties of (PVP-PEG) Blend", Research Journal of Cell and Molecular Biology5, 15-18, (2015).

43. J. D. Thomas, "Novel Associated PVA/PVP Hydrogels for Nucleus Pulposus Replacement", M.Sc. Thesis, Faculty of Drexel University, (2001).

44. F. A. Mustafa, "The Structural and Optical Characteristics of polyvinyl Pyrrolidone Doped with Nano Crystal NaF Films", Natural and Applied Sciences4, 125-141, (2013).

45. J. E. Mark, "Polymer Datahand book", Oxford University Press, Oxford, (1999).

46. C.M. Hassan and N. A. Peppas, "Structure and Applications of (Polyvinyl Alcohol) Hydrogels Produced by Conventional Crosslinking or by Freezing/Thawing Methods" Advances in Polymer Science153,37-65, (2000).

47. H. M. Almamouri and K. Alsultagem."Effect of chlorophyll dye on hardness and damping properties of natural rubber and protection from radiation UV" University of Karbala Scientific Journal.Vol. 7, No.1,(2009).

48. M. H. Al-Mamouri, K. F. Al-Sultani and M. N. Obaid, "Effect Chlorophyll Pigment on Specific Gravity And Tensile Properties For Natural Rubber And Protect It From UV Ray", Engineering and Technology Journal, 27(15), (2009).

49. M. Chen, "Chlorophylls d and f: Synthesis, occurrence, light-harvesting, and pigment organization in chlorophyll-binding protein complexes", In Advances in botanical research, Academic Press , Vol. 90, pp. 121-139, (2019).

50. A. M. El Sayed,S. El-Gama, W. M. Morsi, Gh. Mohammed," Effect of PVA and copper oxide nanoparticles on the structural, optical, and electrical properties of carboxymethyl cellulose films",J Mater Sci. Springer (2015).

51. K. J. Kadhim, I. R.Agool and A. Hashim, Enhancement in Optical Properties of (PVA-PEG-PVP) Blend By the Addition of Titanium Oxide Nanoparticles for Biological Application, Advances in Environmental Biology,Vol.10,pp.81-87,(2016).

52. G.R.Bella, R.S.JebaJ. and T. B. S. Avila ,"Polyvinyl alcohol/Starch/Carboxymethyl cellulose ternary polymer blends: Synthesis, Characterization and Thermal properties" ,Int. J. Current Research in Chemistry and Pharmaceutical Sciences, Vol.3, No.6, pp.43-50 (2016).

53. A. Goswami, A. Bajpai, J. Bajpai, and B. Sinha, “Designing vanadium pentoxide - carboxymethyl cellulose / polyvinyl alcohol - based bionanocomposite films and study of their structure, topography, mechanical, electrical and optical behavior,” Polym. Bull., vol. 75, no. 2, pp. 781–807, (2018).

54. K. Al-Attiyah, A. Hashim, and S. Obaid, “Synthesis of new nanocomposites: Carboxy methyl cellulose–polyvinylpyrrolidone–polyvinyl alcohol/lead oxide nanoparticles: Structural and electrical properties as gamma ray sensor for bioenvironmental applications,” J. Bionanoscience, vol. 12, no. 2, pp. 1–6, (2018).

55. K. Al-Attiyah, A. Hashim, and S. Obaid, “Fabrication of novel (carboxy methyl cellulose–polyvinylpyrrolidone–polyvinyl alcohol)/lead oxide nanoparticles: structural and optical properties for gamma rays shielding applications,” Int. J. Plast. Technol., vol. 23, no. 1, pp. 39–45, (2019).

56. Abid, S. Al-Nesrawy, and A. Abdulridha, “Synthesis Characterization of (PVA- PVP-CB) nano composites,” vol. 7, no. 15, pp. 2524–2532, (2020).

57. M. S. Toman and S. H. Al-nesrawy. "New Fabrication (PVA-CMC-PbO) Nanocomposites Structural and Electrical Properties." NeuroQuantology 19.4: 38,(2021).

58. A. A. Al-Muntaser, R. A. Pashameah , K. Sharma, , E. Alzahrani , S. T.Hameed, and M. A. Morsi, "Boosting of structural, optical, and dielectric properties of PVA/CMC polymer blend using SrTiO3 perovskite nanoparticles for advanced optoelectronic applications", Optical Materials, 132, 112799 , (2022).

59. A. Telser, “Fundamentals of Light Microscopy and Electronic Imaging”, Shock, Vol. 17, No. 5, p. 442, (2002).

60. B. Jörgen, “in Mechanics of Solid Polymers”, (2015).

61. R. Cik, H. Che F. Choo and Azillah Fatimah Othman Nor. "Field Emission Scanning Electron Microscope (FESEM) Facility in BTI." (2015).

62. P. Gnauck, V. Drexel, and J. Greiser, "A New high resolution field emission scanning electron microscope with variable pressure capabilities", Micrsocopy and Microanalysis, 7 : 880 (2001).

63. D.C. Joy and J.B. Pawley, "High resolution scanning electron microscopy", Ultra microscopy, 47: 80-100, (1993) .

64. A.V. Crewe and P.S.D Lin, "Production of a field emission source", In Progress in Optics XI (Eds. Wolf E.) North Holland : 225-246, (1973).

65. J. Pawley, and H. Schatten, (Eds.), "Biological low-voltage scanning electron microscopy", Springer Science and Business Media(2007).

66. M. F. AL-Mudhaffer, M. A. Nattiq and M. Ali Jaber, "Linear optical properties and energy loss function of Novolac: Epoxy blend film", Scholars Research Library, Archives of Applied Science Research, Vol. 4, No. 4, PP.1731-7140(2012).

67. M. S. Toman, and S. H. Al-nesrawy, "New Fabrication (PVA-CMC-PbO) Nanocomposites Structural and Electrical Properties", NeuroQuantology, *19*(4), 38, (2021).

68. A. Ramírez-hernández, C. Aguilar-flores, and A. Aparicio-saguilán, "Fingerprint analysis of FTIR spectra of polymers containing vinyl análisis en la huella dactilar de espectros FTIR de polímeros que contienen etileno," Rev. DYNA, vol. 86, no. 209, pp. 198–205, (2019).

69. P. Q. Rodríguez and Margarita "Fourier transform infrared (FTIR) technology for the identification of organisms" Clinical Microbiology Newsletter, Vol.22, No.8, pp.57-61, (2000).

70. K. Zhang, L.L. Zhang, X.S. Zhao and J. Wu, "Graphene /Polyaniline Nanofiber Composites as Supercapacitor Electrodes", Chem. Mater. 1392–1401 22, (2010).

71. J.D. Wuest, A. Rochefort, "Strong adsorption of aminotriazines on grapheme", Chem. Commun, 2923 46, (2010).

72. Y. Xu, Z. Lin, X. Huang, Y. Wang, Y. Huang and X. Duan, "Functionalized Graphene Hydrogel-Based High-Performance Supercapacitors", Adv. Mater,5779–5784 25, (2013).

73. Y. Lu, Y. Huang, F. Zhang, L. Zhang, X. Yang, T. Zhang, K. Leng, M. Zhang and Y. Chen, "Functionalized graphene oxide based on p-phenylenediamine as spacers and nitrogen dopants for high performance supercapacitors", Chinese Sci. Bull, 1809–1815, 59 (2014).

74. Y. Cui, Q.-Y. Cheng, H. Wu, Z. Wei and B.-H. Han, "Graphene oxide-based benzimidazole-crosslinked networks for high-performance supercapacitors, Nanoscale", 8367, 5 (2013).

75. D.C. Giancoli,"Physics for scientists and engineers with modern physics, Pearson Education", (2008).

76. M. Qiu, Y. Zhang, B. Wen, "Facile synthesis of polyaniline nanostructures with effective electromagnetic interference shielding performance", J. Mater. Sci. Mater. Electron, 10437–10444, 29 (2018).

77. D. I. Bower, "An introduction to polymer physics", (2003).

78. A. Abdulmitalib, "Studying in Electric and Optical Properties of Polymers with Application on Non crystal Films from Poly acrylic acid",M.Sc. Thesis,Collage of Sci, University of Bassrah, (1981).

79. R. T. Kivaisi, "Optical properties of obliquely evaporated aluminium films", Thin Solid Films, Vol. 97, No. 2, pp. 153–163, (1982).

80. G. K. Raheem, S. H. Ahmed, "Study Of Optical Properties Of (PEO-PEG) Blends", Journal University of Kerbala, Vol.12, No. 2, pp.163-174,(2016).

81. M. Stamm, "Introduction to Physical Polymer Science",pp.787-78, (2006).

82. R. Berglund, P. Graham and R. Miller, "Applications of In-situ FT-IR in Pharmaceutical Process R and D", spectroscopy-Springfield then Eugene-, Vol. 8, pp.31-31,(1993).

83. L. A. Prystaj,"effect of carbon filler characteristics on the electrical properties of conductive polymer composites possessing segregated network microstructures", M.Sc.E. Thesis, Georgia Institute of Technology , (2008).

84. C. Kittel, "Introduction to solid state physics", 5th Ed, Willy, New York, (1981).

85. F. Yakuphanoglu and H. Erten, “Refractive index dispersion and analysis of the optical constants of an ionomer thin film”,Optica applicata, Vol. 35, No. 4, pp. 969–976, (2005).

86. H. A. Macleod, “Thin Film Optical Filter”, McGraw-Hill, New York. (2001).

87. O. G. Abdullah, B. K. Aziz, and S. A. Hussen, “Optical Characterization of Polyvinyl alcohol - AmmoniumNitrate Polymer Electrolytes Films”, Journal of Chemistry and Materials Research, Vol. 3, No. 9,pp.84-90,(2013).

88. A. V. Vannikov, V. K. Matveev, V. P. Sichkar, and A. P. Tiutnev, “Radiation effects in polymers, Electrical properties,” Moscow Izd. Nauk, (1982).

89. K. H. Abass and D. M. Latif. “The urbach energy and dispersion parameters dependence of substrate temperature of CdO thin films prepared by chemical spray pyrolysis”, International Journal of ChemTech Research, Vol. 9, No. 9,pp.332-338, (2016).

90. J. I. Pankove, “Optical Process in Semiconductors”, Dover Publishing, Inc., New York, (1971).

91. A. N. Donald, “Semiconductor physics and devices”, Irwin, University of New Mexico, USA, (1992).

92. A. N. Alias, Z. M. Zabid, A. M. M. Ali, M. K. Harun, and M. Z. A. Yahya, “Optical Characterization and Properties of Polymeric Materials for Optoelectronic and Photonic Applications,” Int. J. Appl. Sci. Technol., Vol. 3, No. 5, pp. 11–38, (2013).

93. R. Naik, C. Kumar, R. Ganesan, and K. S. Sangunni, “Effect of Thickness on The Optical Properties Change in Bi / As 2S3 Bilayer Thin Films,” Chem. Mater. Res., Vol. 6, No. 2, pp. 1–2, (2014).

94. V. N.Suryawanshi, A. S. Varpe, M. D. Deshpande, “Band gap engineering in PbO nanostructured thin films by Mn doping”, Thin Solid Films, Vol. 645, pp. 87-92. (2018).

95. C. Mwolfe, N.Holouyak,and G.B.Stillman, “Physical Properties of Semiconductor”, prentice Hall, New York, (1989).

96. Y. N. Al-Jamal, “Solid State Physics”, Al-Mosel University, (2nd Ed.), Arabic Version, (2000).

97. T. Numai, “Fundamentals of semiconductor lasers: Second edition” , Springer Ser. Opt. Sci, Vol. 93, No.28 Augst, pp.55147, (2015).

98. J. Pankove and D. Kiewit, “Optical Processes in Semiconductors”, Electrochemist. Soc, Vol. 119, No. 5, pp.156C, (1972).

99. N. Rangelova, L. Aleksandrov, T. Angelova, N. Georgieva and R. Muller,"Carbohydr. Polym", 101, 1166–1175 ,(2014).

100. S. Mallakpour, F. Motirasoul, Prog. Org. Coat. 103, 135–142, (2017).

101. M. Yu, , Y. Han, , J. Li, , and L. Wang, "Three-dimensional porous carbon aerogels from sodium carboxymethyl cellulose/poly (vinyl alcohol) composite for high-performance supercapacitors", Journal of Porous Materials, 25, 1679-1689,(2018).

102. M. El-Bana, G. Mohammed, A.M. El Sayed and S. El-Gamal, "Preparation and characterization of PbO/carboxymethyl cellulose/ polyvinylpyrrolidone nanocomposite films", Polym. Compos. 39, 3712–3725, (2017).

103. M. A. Morsi, , A. Rajeh, and A. A. Menazea, "Nanosecond laser-irradiation assisted the improvement of structural, optical and thermal properties of polyvinyl pyrrolidone/carboxymethyl cellulose blend filled with gold nanoparticles", Journal of Materials Science: Materials in Electronics, 30, 2693-2705, (2019).

104. S. D. Meshram, R. Rupnarayan, S. V. Jagtap, V. G. Mete and V. S. Sangawar, "Synthesis and Characterization of Lead Oxide Nanoparticles", International Journal of Chemical and Physical Sciences, Vol. 4, Special Issue, PP. 83-88, (2015).

105. M. I. H. A. Sohaimy, and M. I. N. M. Isa, "Natural inspired carboxymethyl cellulose (CMC) doped with ammonium carbonate (AC) as biopolymer electrolyte" Polymers, Vol. 12, No.11, p. 2487, (2020).

106. M. A. Morsi, A. H. Oraby, A. G. Elshahawy, and R. M. Abd El-Hady, " Preparation, structural analysis, morphological investigation and electrical properties of gold nanoparticles filled polyvinyl alcohol/carboxymethyl cellulose blend" Journal of materials research and technology, Vol. 8, No. 6, pp.5996-6010, 2019)).

107. M. A. Morsi, A. Rajeh and A. A. Menazea, "Nanosecond laser-irradiation assisted the improvement of structural, optical and thermal properties of polyvinyl pyrrolidone/carboxymethyl cellulose blend filled with gold nanoparticles" Journal of Materials Science: Materials in Electronics, Vol. 30, pp. 2693-2705, 2019)).

108. M. Morsi, M. Abdelaziz, A. Oraby, I. Mokhles, "Effect of lithium titanate nanoparticles on the structural, optical, thermal and electrical properties of polyethylene oxide/carboxymethyl cellulose blend" J. Mater. Sci.: Mater. Electron, Vol. 29, No. 18, pp. 15912–15925, (2018)

109. I. Tittonen, "Improving the optical properties of chlorophyll aggregates with supramolecular design (Doctoral dissertation)", Aalto University, (2011).

110. L. Chaudhari and R. Nathuram, " Absorption Coefficient of Polymers (Polyvinyl Alcohol) by Using Gamma Energy of 0.39MeV", Bulg. Journal of Physics, Vol. 37, PP. 232–240,(2010)

111. S. Kolpakov, N. Gordon, C. Mou, and K. Zhou, " Toward a New Generation of Photonic Humidity Sensors", Journal of Sensors, Vol.14, PP. 3986-4013; doi:10.3390/s140303986, (2014).

112. N. D. Md Sin, M. F. Tahar, M. H. Mamat and M. Rusop, "Enhancement of Nanocomposite for Humidity Sensor Application", Journal of Recent Trends in Nanotechnology and Materials Science, Engineering Materials, DOI: 10.1007/978-3-319- 04516-0_2, P. 15-31, PP. 15-30,(2014).

113. O. Abdullah, D. R. Saber and L. O. Hamasalih, "Complexion Formation in PVA/PEO/CuCl2 Solid Polymer Electrolyte", Universal Journal of Materials Science, Vol. 3, No. 1, PP.1-5, (2015)

114. N. B. Rithin Kumar, V. Crasta, R. F. Bhajantri and B.M. Praveen, "Microstructural and Mechanical Studies of PVA Doped with ZnO and WO3 Composites Films", Journal of Polymers, Vol. 2014, P.7, (2014).

115. J. Ramesh Babu and K. Vijaya Kumar, "Studies on Structural and Electrical Properties of NaHCO3 Doped PVA Films for Electrochemical Cell Applications", International Journal of Chem. Tech. Research, Vol.7, No. 1, PP.171-180, (2014).

116. S.H. Borova, O.M. Shevchuk, N.M. Bukartyk, E.Yu. Nikitishyn and V. Tokarev, "Nanocomposite Films Based on Functional Copolymers with Embedded Carbon Nanotubes", proceedings of the International Conference Nanomaterials: Applications and Properties, Vol. 3, No. 2, (2014).

117. S. Salman, N. Bakr and M. H. Mahmood, "Preparation and study of some optical properties of (PVA- Ni(CH3COO)2) composites", International Journal of Current Research, Vol. 6, No.11, pp.9638-9643, (2014).

118. A. Mohammad, K. Hooshyari, M. Javanbakht, and M. Enhessari, "Fabrication and Characterization of Poly Vinyl Alcohol/ Poly Vinyl Pyrrolidone/MnTiO Nanocomposite Membranes for PEM Fuel Cells", Iranica Journal of Energy & Environment, Vol. 4, No. 2, PP. 86-90 , (2013).

119. K. Karthikeyan, N. Poornaprakash, N. Selvakumar and Jeyasubrmanian, "Thermal Properties and Morphology of MgO-PVA Nanocomposite Film", Journal of Nanostructured Polymers and Nanocomposites, Vol. 5, No. 4, PP. 83-88, (2009).

120. N. Elmarzugi1, T. Adali, A. Bentaleb, E. I. Keleb, A. T. Mohamed and A. M. Hamza, " Spectroscopic Characterization of PEG- DNA Biocomplexes by FTIR", Journal of Applied Pharmaceutical Science, Vol. 4, No. 8, PP. 6-10, (2014).

121. N. Arsalani, H. Fattahi and M. Nazarpoor, " Synthesis and characterization of PVP-functionalized superparamagnetic Fe3O4 nanoparticles as an MRI contrast agent", Journal of eXPRESS Polymer Letters Vol.4, No.6, PP. 329–338,(2010).

122. D. Kumar, S. Karan Jat, P. K. Khanna, N. Vijayan, S. Banerjee, "Synthesis, Characterization, and Studies of PVA/Co-Doped ZnO Nanocomposite Films", International Journal of Green Nanotechnology, Vol. 4, PP.408–416,(2012).

123. C. Srikanth, C. Sridhar, B. M. Nagabhushana and R.D.Mathad,"Characterization and DC Conductivity of Novel CuO doped Polyvinyl Alcohol (PVA) Nano-composite Films", Journal of Engineering Research and Applications, Vol. 4, Issue 10, pp..38-46,(2014).

124. A. A Abid, S. H. Al-nesrawy , and A. R. Abdulridha, "New fabrication (PVA-PVP-C. B) nanocomposites: structural and electrical properties", In Journal of Physics: Conference Series (Vol. 1804, No. 1, p. 012037) IOP Publishing, February , (2021).

125. G.H. Murhekar and A.R. Raut, " Electrical properties of modified polyvinyl alcohol conjugates and doped modified polyvinyl alcohol conjugates", International Journal of Chemical Studies, Vol. 2, Issue 2, PP. 77-82, (2014).

الخلاصة

في هذه الدراسة ، تم تحضير المتراكب النانوي (CMC / PVA / Mg-Chlorophyll) و (CMC / PVP / Mg-Chlorophyll) باستخدام طريقة الصب وبتراكيز مختلفة من Mg-Chlorophyll nanoparticles بنسب وزنية (2, 4 , 6 , 8) % . تم دراسة الخصائص التركيبية والمورفولوجيا والبصرية للمركب النانوي (CMC / PVA / Mg-Chlorophyll) و (CMC / PVP / Mg-Chlorophyll). تشمل الخصائص التركيبية حيود الأشعة السينية (XRD) ، والمجهر البصري (OM) ، ومجهر المسح الإلكتروني لانبعاث المجال (FESEM) والأشعة تحت الحمراء لتحويل فوريير (FTIR).

فحص XRD اظهر أن التركيب شبه البلوري لمزيج بوليمر CMC / PVA و CMC / PVP ومع إضافة تركيز مختلف من أصباغ Mg-Chlorophyll بنسب (4,2 , 6 , 8)% ، زادت الكثافة ولا تظهر أي قمم ، بسبب التركيز المنخفض المضاف إلى مزيج بوليمر CMC / PVA و CMC / PVP وأيضًا بسبب القمم الواسعة لـ CMC / PVA و CMC / PVP التي تختفي جميع القمم.

فحص المجهر البصري و FESEM ، ظهرت الصور أن (Mg-Chlorophyll) تشكل شبكة مستمرة داخل مزيج بوليمر CMC / PVA و CMC / PVP بتركيز 8٪ بالوزن .

يُظهر أطياف FTIR تحولًا في بعض الروابط وتغيرًا في الشدة وأثبت أنه لا توجد تفاعلات بين مصفوفة بوليمر CMC / PVA و CMC / PVP والجسيمات النانوية Mg-Chlorophyll. أظهرت الخواص البصرية أن الامتصاصية ، ومعامل الامتصاص ، ومعامل الانقراض ، ومعامل الانكسار ، والأجزاء الحقيقية والخيالية من ثوابت العزل والتوصيل البصري تزداد بزيادة تركيز جسيمات Mg-Chlorophyll النانوية ، بينما تقل النفاذية وفجوة الطاقة غير المباشرة مع زيادة تركيز جسيمات Mg-Chlorophyll النانوية. زيادة تركيز الجسيمات النانوية المالئة Mg-Chlorophyll .

تطبيق هذه الدراسة هو لتوهين الموجات الكهرومغناطيسية للمتراكب النانوي (CMC / PVA / Mg-Chlorophyll) و (CMC / PVP / Mg-Chlorophyll) .

جمهورية العراق
وزارة التعليم العالي والبحث العلمي
جامعة بابل ـ كلية التربية للعلوم الصرفة
قسم الفيزياء

تحضير المادة المالئة الحيوية الكلوروفيل دراسة تأثيرها على الخواص التركيبية والبصرية لبعض الخلائط البوليمرية الحيوية

رسالة مقدمة

إلى مجلس كلية التربية للعلوم الصرفة في جامعة بابل وهي جزء من متطلبات

نيل درجة الماجستير في التربية / الفيزياء

من قبل

أحمد حسين عرار كاظم

بكالوريوس تربية علوم(فيزياء)

جامعة بابل 2009 م

بإشراف

أ. د. سمير حسن هادي النصراوي

1445 هـ **2023 م**